



Geological Survey of Canada

CURRENT RESEARCH  
2003-F2

**SHRIMP U-Pb detrital zircon  
geochronology of Athabasca Group  
sandstones, northern Saskatchewan  
and Alberta**

*N.M. Rayner, R.A. Stern, and R.H. Rainbird*

2003



Natural Resources  
Canada

Ressources naturelles  
Canada

Canada

CURRENT RESEARCH

©Her Majesty the Queen in Right of Canada 2003  
ISSN 1701-4387  
Catalogue No. M44-2003/F2E-PDF  
ISBN 0-662-35069-3

A copy of this publication is also available for reference by depository libraries across Canada through access to the Depository Services Program's website at <http://dsp-psd.pwgsc.gc.ca>

A free digital download of this publication is available from the Geological Survey of Canada Bookstore web site:

<http://gsc.nrcan.gc.ca/bookstore/>

Click on Free Download.

**All requests for permission to reproduce this work, in whole or in part, for purposes of commercial use, resale, or redistribution shall be addressed to: Earth Sciences Sector Information Division, Room 402, 601 Booth Street, Ottawa, Ontario K1A 0E8.**

### **Authors' addresses**

*N. Rayner (nrayner@nrcan.gc.ca)*

*R.A. Stern (rstern@cmm.uwa.edu.au)*

*R.H. Rainbird (rrainbir@nrcan.gc.ca)*

*Continental Geoscience Division*

*Geological Survey of Canada*

*Natural Resources Canada*

*601 Booth Street*

*Ottawa, Ontario K1A 0E8*

Publication approved by Continental Geoscience Division

# SHRIMP U-Pb detrital zircon geochronology of Athabasca Group sandstones, northern Saskatchewan and Alberta<sup>1</sup>

*Rayner, N.M., Stern, R.A., and Rainbird, R.H., 2003: SHRIMP U-Pb detrital zircon geochronology of Athabasca Group sandstones, northern Saskatchewan and Alberta; Geological Survey of Canada, Current Research 2003-F2, 20 p.*

---

**Abstract:** Detrital zircon geochronology was conducted on five sandstone units from the Athabasca Group of northern Saskatchewan and Alberta using the SHRIMP II ion microprobe. In ascending stratigraphic order, the youngest zircons from the Fair Point Formation and from members B and D of the Manitou Falls Formation yielded maximum ages of deposition of  $1810 \pm 15$  Ma,  $1819 \pm 21$  Ma, and  $1814 \pm 23$  Ma, respectively. The overlying Wolverine Point Formation yielded three zircons with a mean age of  $1662 \pm 17$  Ma. Among the five samples studied, these zircons are the youngest encountered and provide the best constraint on the maximum age of the upper part of the Athabasca Group. The youngest zircons from the uppermost Douglas Formation range in age from 1775 to 1765 Ma. The key age modes identified from the five samples are 1780 Ma, 1850 Ma, 1900 Ma, 2530 Ma, 2580 Ma, 2610 Ma, and ca. 2700 Ma.

**Résumé :** Au moyen de la microsonde ionique SHRIMP II, on a pu établir la géochronologie U-Pb sur zircon détritique de cinq grès appartenant au Groupe d'Athabasca, dans le nord de la Saskatchewan et de l'Alberta. En ordre stratigraphique croissant, les zircons les plus récents extraits de la Formation de Fair Point et des membres B et D de la Formation de Manitou Falls ont livré des âges maximaux de dépôt de  $1810 \pm 15$  Ma,  $1819 \pm 21$  Ma et  $1814 \pm 23$  Ma, respectivement. Trois zircons de la Formation de Wolverine Point sus-jacente ont livré un âge moyen de  $1662 \pm 17$  Ma. Parmi tous les échantillons analysés, ces trois zircons sont les plus récents; ce sont eux qui ont le mieux permis d'encadrer l'âge maximal de la partie supérieure du Groupe d'Athabasca. L'âge des plus récents zircons de la partie sommitale de la Formation de Douglas varie de 1775 à 1765 Ma. Dans les diagrammes de fréquences cumulées des âges, les modes les plus marqués pour l'ensemble des échantillons se situent à 1780 Ma, 1850 Ma, 1900 Ma, 2530 Ma, 2580 Ma, 2610 Ma et environ 2700 Ma.

---

<sup>1</sup> Contribution to the Targeted Geoscience Initiative (TGI) 2000–2003.

---

## INTRODUCTION

One objective of the EXTECH IV: Athabasca Uranium Multidisciplinary Study is to enhance, through new regional- and deposit-scale studies, the understanding of both the broad geological environment and the depositional setting of the world-class, unconformity-hosted uranium deposits of the Athabasca Basin (Jefferson et al., 2002). By obtaining profiles of U-Pb SHRIMP ages from detrital zircon samples from a variety of stratigraphic levels, we hope to constrain the timing of deposition and to provide quantitative constraints on a regional provenance model for the Athabasca Group. To date, the provenance of this large (100 000 km<sup>2</sup>) and thick (2300 m) sandstone basin has not been systematically investigated with U-Pb detrital zircon geochronology. Furthermore, relatively few geochronological data constraining sandstone depositional and diagenetic ages are available (Armstrong and Ramaekers, 1985; Cumming et al., 1987; Kotzer and Kyser, 1995). Based on these existing data, the initiation of deposition is poorly constrained to younger than ca. 1800 Ma and sedimentation appears to have continued for at least 150 Ma.

This report is the first of a two-part series on the detrital zircon geochronology of the Athabasca Group. Part one describes the methodology of the detrital zircon study and provides detailed descriptions of the samples and their U-Pb geochronology. Part two, to be published by Rainbird and others in the EXTECH IV final volume, will discuss the provenance of the Athabasca Group, based on the U-Pb ages presented here, and the implications for regional stratigraphic correlation and tectonic evolution of the Athabasca Basin.

---

## SAMPLES AND PETROGRAPHIC DESCRIPTIONS

Five samples of heavy-mineral-bearing Athabasca Group sandstone were collected from localities in Saskatchewan and Alberta: three from widely spaced 'stratigraphic' drillholes and two from outcrop. Samples weighed up to about 2 kg. Sample locations, both geographic and stratigraphic, are illustrated in Figures 1 and 2 and summarized in Table 1. Sample 02JP-12, 13, 14 (lab number z7461) is a sublitharenite to quartz arenite taken from the upper Fair Point Formation. Grain size ranges from coarse to very coarse sand. Sorting is poor to moderate, and grains are angular to subrounded. Ninety-five percent of the clasts are composed of quartz (40% strained, 40% monocrystalline, and 15% polycrystalline) with the remaining 5% of framework grains being miscellaneous rock fragments, including detrital mica. The framework is highly compressed, with extensive pressure solution along grain boundaries. The cement is composed of early quartz overgrowths on detrital quartz as well as ubiquitous clay cement and pseudomatrix that includes chlorite, white mica, and an unidentified mica forming blocky booklets. Figure 3a is a representative photomicrograph of a thin section of this rock.

Sample RAT01-MF1 (z7465) is a quartz arenite from member B of the Manitou Falls Formation, exposed at the haulage ramp in Sue Pit, McClean Lake area, eastern

Athabasca Basin. Grain size is coarse sand. Sorting is poor to moderate, and the clasts are subangular to rounded. The framework is moderately compressed, with common sutured grain boundaries. Ninety-five percent of the clasts are composed of quartz (20% strained, 65% monocrystalline, and 10% polycrystalline), with the remaining 5% of clasts composed of miscellaneous rock fragments, including detrital mica. The cement is composed of early quartz overgrowths on detrital quartz and pore-filling matrix clay, much of which could represent altered rock fragments. Figure 3b is a representative photomicrograph of a thin section of this rock.

Sample 02JP-15a (z7462) is an apatite-impregnated breccia of quartz arenite from outcrop in the Riou Lake area, mapped as the top of member D of the Manitou Falls Formation. Framework grains in the quartz-arenite parent rock are medium- to coarse-sand-sized, well rounded and well sorted. The framework is intact, with minor suturing of grain contacts. The clasts are composed exclusively of quartz (60% strained, 30% monocrystalline, and 10% polycrystalline). The cement is composed of hematite-dust rims defining original grain boundaries, early quartz overgrowths on detrital quartz, diagenetic xenotime overgrowths on detrital zircons, and blocky apatite cement. Hematite is located in cores of apatite-cement crystals, imparting a very dark colour to the apatite cement as well as a rusty brown appearance to hand samples. Late quartz and hematite infill remaining voids. Figure 3c is a representative photomicrograph of a thin section of this rock.

Sample 02JP-7b (z7460), taken from drill core of member B of the Wolverine Point Formation, is a quartz arenite with flat lithic-tuff pebbles. Grain size is coarse to very coarse pebbly sand, sorting is moderate, and grains are moderately to well rounded. The framework is intact, with minor suturing of grain-to-grain contacts. Ninety-five percent of clasts are composed of quartz (40% strained, 50% monocrystalline, and 5% polycrystalline). The remaining 5% of clasts are composed of tuff fragments. The cement comprises early quartz overgrowths on detrital quartz, secondary pore-filling botryoidal chalcedony, and hematite replacement in cement and framework. Figure 3d is a representative photomicrograph of a thin section of this rock.

Sample 02JP-20a (z7464) is interlaminated lithic arenite and lutite from the Douglas Formation in drillhole DGS-04 on the south side of the Carswell Structure. Framework clasts in arenite laminae are fine to very fine sand in size, angular to subangular, and moderately well sorted. Clasts are composed of quartz (60%), dolomite (30%), and feldspar (10%). The cement is composed of quartz overgrowths on detrital quartz grains. Lutite laminae are brown, with mineralogy similar to that of the arenite laminae, but with abundant organic material in the matrix. Figure 3e is a representative photomicrograph of a thin section of this rock.

---

## ANALYTICAL PROCEDURES

SHRIMP analytical procedures are described by Stern (1997), with standards and U-Pb calibration methods following Stern and Amelin (2003). In brief, zircons were cast in a



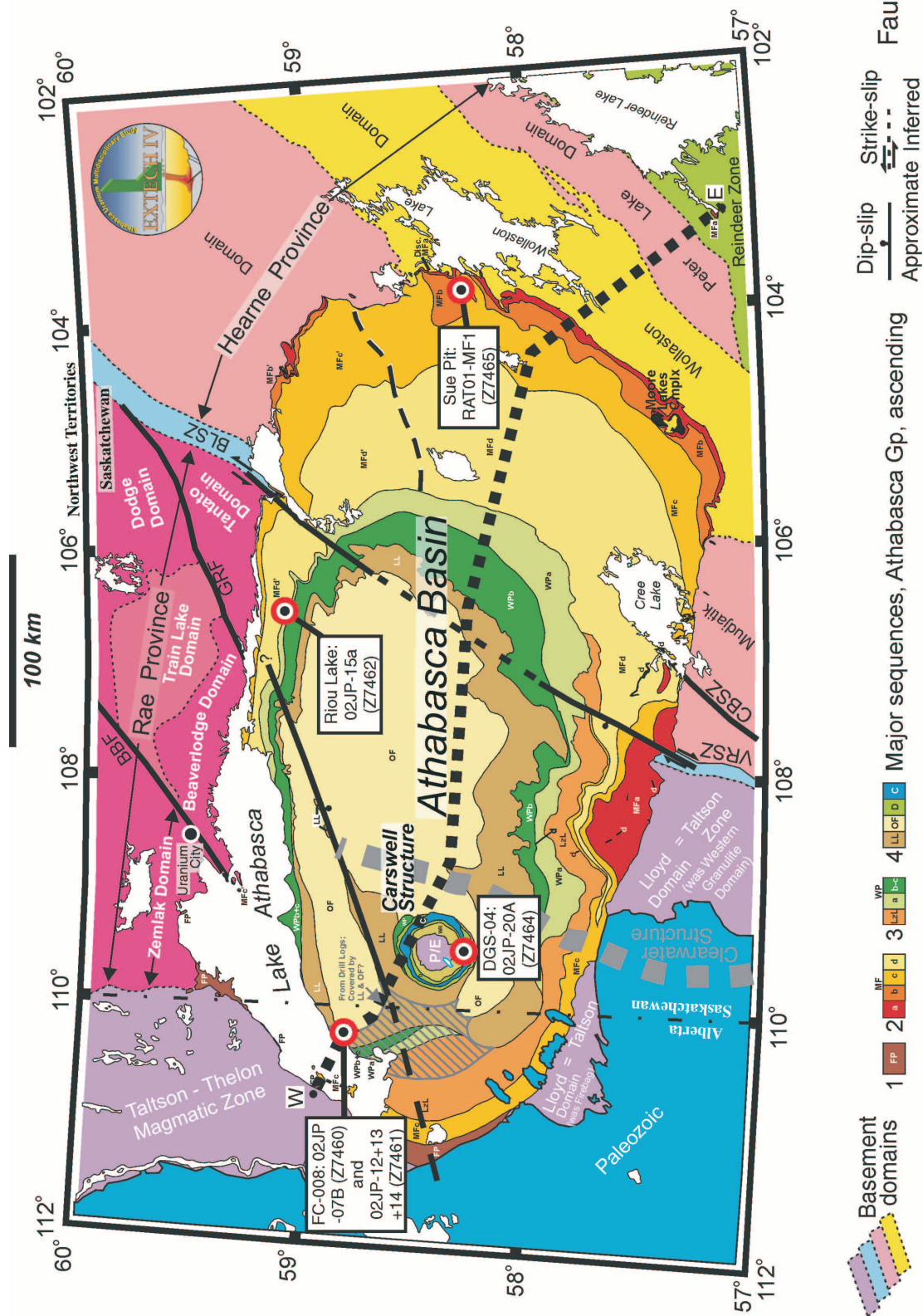


**Figure 1.** Location of detrital zircon samples with respect to major basement domains and stratigraphy of the Athabasca Basin (after Ramaekers et al. 2001 and Thomas et al. 2002). Formations are: FP = Fair Point, MFa through MFd = Manitou Falls, WPa, b = Wolverine Point, LL = Locker Lake, OF = Otherside, WR = undivided William River Subgroup (MF through OF), D = Douglas, C = Carswell. Other rock units are: d = diabase; ML = Moore Lakes gabbro complex; P/E = undivided Peter River / Earl River gneisses in the Carswell Structure. BBF & GRF = Black Bay and Grease River faults; BLSZ, CBSZ & VRSZ = Black Lake, Cable Bay & Virgin River shear zones. Dotted line E-W shows location of cross-section shown in Fig. 2.

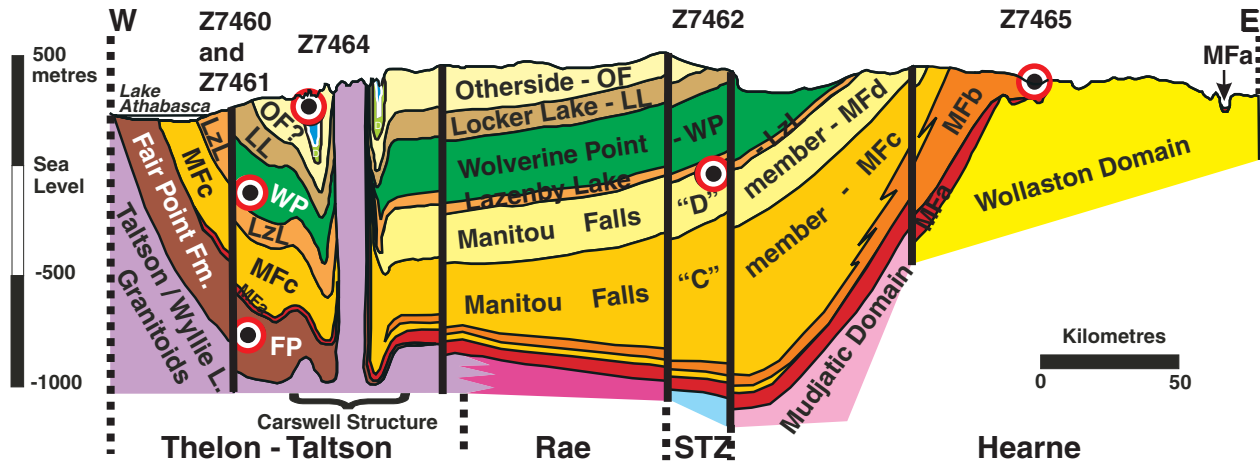


Figure 2. East-west cross-section of Athabasca Basin showing projected drillholes and stratigraphic levels of samples used in this study. STZ = Snowbird Tectonic Zone.

Table 1. Athabasca Basin sample locations.

Sample	Unit	Stratigraphic position	Rock type	Location	UTM		
					Zone	Easting	Northing
z7464 / 02JP-20A	Douglas Fm	top	Lithic arenite	Carswell	12	582440	6463400
z7460 / 02JP-07B	Wolverine Point Fm member B	↑	Quartz arenite	Northwest basin	12	541354	6523361
z7462 / 02JP-15a*	Manitou Falls Fm member D		Quartz arenite	North-central margin	13	414323	6563077
z7465 / RAT01-MF1	Manitou Falls Fm member B		Quartz arenite	Eastern margin	13	605600	6459600
z7461 / 02JP-12,13,14	Fair Point Fm	bottom	Sub-lithic arenite	Northwest basin	12	541354	6523361

\*brecciated apatite-mineralized sandstone from inferred Manitou Falls Formation member D, unconformably overlain by Wolverine Point Formation.

2.5 cm diameter epoxy mount (GSC #IP275) along with fragments of the GSC laboratory standard zircon (z6266, with  $^{206}\text{Pb}/^{238}\text{U}$  age = 559 Ma). The mid-sections of the zircons were exposed using 9, 6, and 1  $\mu\text{m}$  diamond compound, and internal features of the zircons (such as zoning, structures, alteration, etc.) were characterized with backscattered electrons (BSE) using a Cambridge Instruments scanning electron microscope. Mount surfaces were evaporatively coated with 10 nm of high-purity Au. Most analyses were conducted using an  $\text{O}^-$  primary beam, projected onto the zircons at 10 kV as an elliptical spot approximately 35  $\mu\text{m}$  in diameter with a beam current of 9 to 12 nA and uniform density; however, some analyses on small and altered grains were conducted using a spot approximately 20  $\mu\text{m}$  in diameter with an  $\text{O}^-$  primary beam current of about 4 nA. The count rates of ten isotopes of  $\text{Zr}^+$ ,  $\text{U}^+$ ,  $\text{Th}^+$ , and  $\text{Pb}^+$  in zircon were sequentially measured (4 or 5 scans) with a single electron multiplier and a pulse-counting system with deadtime of 24 ns. Mass resolution was 5050 (1%). Off-line data processing was accomplished using customized in-house software. The  $1\sigma$  external errors for the  $^{206}\text{Pb}/^{238}\text{U}$  ratios reported in Table 2 incorporate a  $\pm 1.0$  to 1.3% error in calibrating the standard zircon (see Stern and

Amelin, 2003). No fractionation correction was applied to the Pb-isotope data. Isoplot v. 2.49 (Ludwig, 2001) was used to generate concordia plots and calculate weighted means.

## RESULTS

### z7461 Fair Point Formation

A representative sample of zircons from sample z7461 is shown in Figure 4a. In plane light, the zircons appear to be of fair to poor quality; the majority of grains are dark brown and moderately to highly turbid. Scanning electron microscope images reveal little alteration, despite the turbid and fractured appearance of the grains. The zircon sample can be subdivided into four broad morphologies: 1) Prismatic, subrounded, colourless to medium brown zircons with clarity varying from good to poor. One example is grain 104 (see Fig. 4a, b). Backscattered electron images of these zircons reveal faint concentric zoning and their highly fractured nature. Some zircons contain large inclusions (black spots in BSE image). Mild to moderate alteration is recognized as dark grey areas that parallel or transect the zoning. 2) Dark



brown, highly turbid and fractured grains, typically well rounded with one fractured end (*see* Fig. 4, grain 69). Back-scattered electron images reveal that these zircons are generally unzoned or exhibit patchy zonation and are highly fractured. 3) A minor number of zircons are very clear and colourless, most of these being fragmented with one well rounded surface (*see* Fig. 4, grain 95). In BSE images, these zircons exhibit broad concentric zoning and are not internally

fractured. 4) Angular fragments, which may simply be the result of lab processing, are the final morphology recognized. In BSE images, many of these zircons are unzoned; some exhibit patchy irregular zoning. They are commonly highly fractured and exhibit some alteration (*see* Fig. 4, grain 3).

Sixty-seven analyses were conducted on 61 different zircon grains. The results are plotted in Figure 5 on a concordia diagram and a cumulative probability curve with overlain

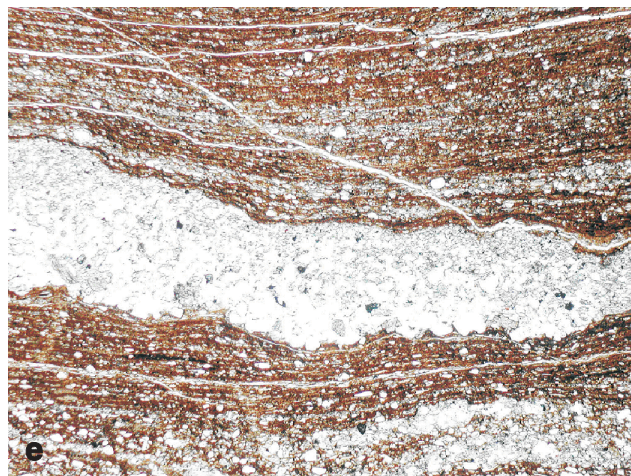
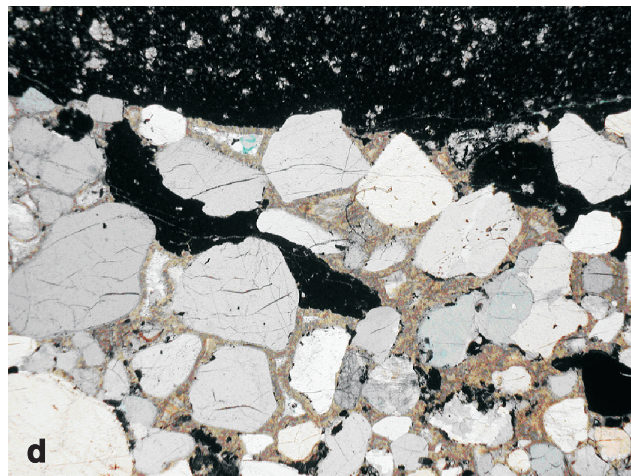
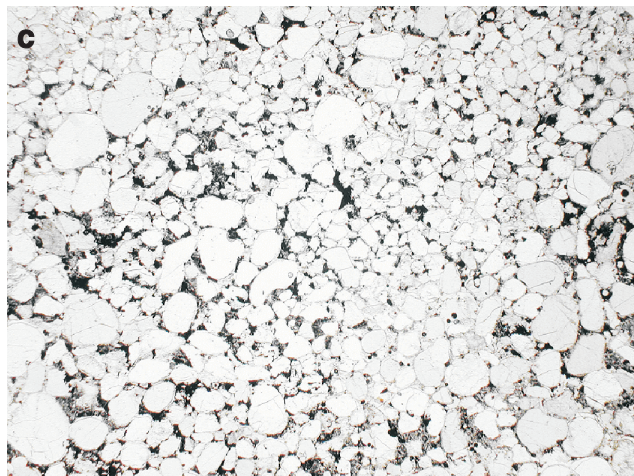
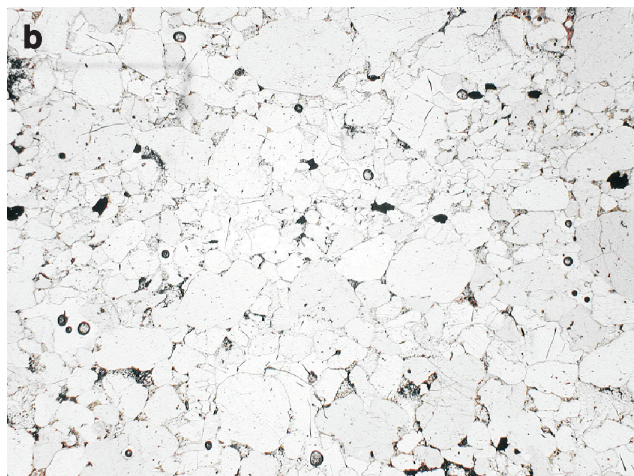
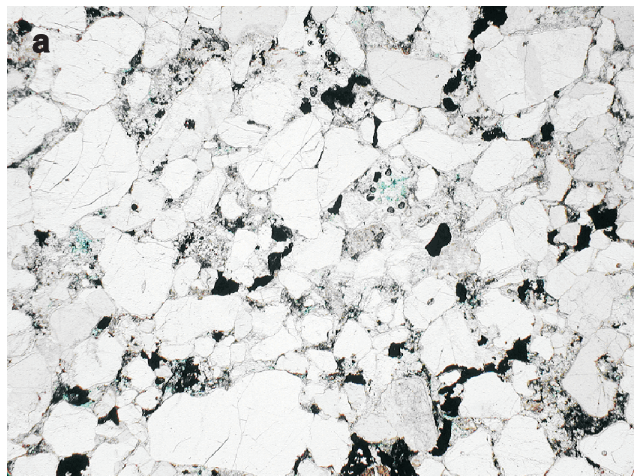


**Figure 3.**

*Photomicrographs of the samples studied. a) z7461 (Fair Point Formation); plane-polarized light; field of view = 6 mm. b) z7465 (Manitou Falls Formation, member B); plane-polarized light; field of view = 6 mm. c) z7462 (brecciated, apatite-mineralized Manitou Falls Formation, member D); plane-polarized light; field of view = 6 mm. d) z7460 (Wolverine Point Formation, member B); crossed polars; field of view = 6 mm. e) z7464 (Douglas Formation); plane-polarized light; field of view = 3 mm.*



**Table 2. SHRIMP U-Pb results from Athabasca Basin detrital zircons. Errors are reported at 1 sigma level.**

Spot name	U (ppm)	Th (ppm)	Th/U	Pb* (ppm)	<sup>204</sup> Pb (ppb)	<sup>206</sup> Pb/ <sup>208</sup> Pb	$\pm \frac{206}{208} \text{Pb}$	$f(206)^{204}$	$\frac{206}{208} \text{Pb}$ / $\frac{206}{208} \text{Pb}$	$\pm \frac{206}{208} \text{Pb}$	$\frac{207}{206} \text{Pb}$ / $\frac{207}{206} \text{Pb}$	$\pm \frac{207}{206} \text{Pb}$	Corr. coeff.	Apparent ages (Ma)				Disc. (%)				
														$\frac{206}{208} \text{Pb}$ / $\frac{206}{208} \text{Pb}$	$\pm \frac{206}{208} \text{Pb}$	$\frac{207}{206} \text{Pb}$ / $\frac{207}{206} \text{Pb}$	$\pm \frac{207}{206} \text{Pb}$					
z7464 Douglas Formation																						
7464-9.1	93	30	0.34	29	2	9.71E-05	5.26E-05	0.00168	0.0896	0.0027	4.571	0.101	0.3070	0.0049	0.7897	0.1080	0.0015	1726	24	1766	25	2.3
7464-9.2	79	23	0.30	25	1	6.55E-05	3.88E-05	0.00113	0.0802	0.0021	4.664	0.093	0.3054	0.0049	0.8686	0.1108	0.0011	1718	24	1812	18	5.2
7464-9.1.2	90	27	0.31	28	2	8.31E-05	5.63E-05	0.00144	0.0836	0.0032	4.543	0.123	0.2999	0.0060	0.8146	0.0017	0.0011	1691	30	1797	29	5.9
7464-15.1	223	69	0.32	69	9	1.64E-04	4.31E-05	0.00284	0.0858	0.0022	4.445	0.069	0.3014	0.0033	0.7932	0.1070	0.0010	1698	17	1748	17	2.9
7464-15.1.2	261	93	0.37	75	12	1.87E-04	5.41E-05	0.00324	0.0931	0.0032	4.227	0.074	0.2766	0.0038	0.8389	0.1108	0.0011	1574	19	1813	18	13.2
7464-56.1	145	32	0.23	46	0	1.00E-05	1.00E-05	0.00017	0.0681	0.0019	4.644	0.099	0.3117	0.0039	0.6769	0.1081	0.0017	1749	19	1767	29	1
7464-4.1	221	50	0.24	69	0	4.74E-06	2.96E-05	0.00008	0.0700	0.0019	4.581	0.079	0.3074	0.0044	0.8666	0.1081	0.0009	1728	22	1767	15	2.2
7464-49.1	159	46	0.30	51	2	4.85E-05	2.33E-05	0.00084	0.0807	0.0016	4.663	0.083	0.3125	0.0046	0.8809	0.1082	0.0009	1753	23	1770	16	0.9
7464-19.1	306	86	0.29	92	9	1.20E-04	3.18E-05	0.00208	0.0834	0.0032	4.387	0.084	0.2992	0.0045	0.7922	0.1085	0.0014	1657	22	1775	24	6.6
7464-43.1	153	54	0.36	47	1	2.96E-05	2.89E-05	0.00051	0.1023	0.0021	4.441	0.082	0.2953	0.0044	0.8737	0.1091	0.0010	1668	22	1784	17	6.5
7464-20.1	236	30	0.13	71	5	7.86E-05	3.33E-05	0.00136	0.0943	0.0024	4.615	0.088	0.3067	0.0034	0.8260	0.1092	0.0009	1724	17	1785	15	3.4
7464-16.1	223	66	0.30	68	5	9.54E-05	4.26E-05	0.00165	0.0820	0.0023	4.496	0.073	0.2982	0.0034	0.7803	0.1094	0.0011	1682	17	1789	19	5.9
7464-13.1	176	99	0.58	62	3	5.47E-05	3.08E-05	0.00095	0.1688	0.0027	4.798	0.088	0.3174	0.0047	0.8781	0.1096	0.0010	1777	23	1793	16	0.9
7464-28.1	102	34	0.35	32	3	1.14E-04	5.49E-05	0.00197	0.0999	0.0031	4.593	0.095	0.3013	0.0042	0.7545	0.1106	0.0015	1698	21	1809	25	6.1
7464-3.1	141	96	0.71	45	19	5.62E-04	8.64E-05	0.00975	0.1980	0.0042	4.314	0.110	0.2820	0.0053	0.8094	0.1110	0.0017	1601	27	1816	28	11.8
7464-33.1	201	44	0.23	62	3	4.89E-05	3.04E-05	0.00085	0.0641	0.0016	4.666	0.083	0.3045	0.0045	0.8929	0.1111	0.0009	1714	22	1818	15	5.7
7464-5.1	146	240	1.41	79	2	3.89E-05	1.92E-05	0.00067	0.3943	0.0037	4.917	0.087	0.3196	0.0047	0.8895	0.1116	0.0009	1788	23	1826	15	2.1
7464-8.1	176	56	0.39	49	1	1.99E-05	3.30E-05	0.00034	0.1236	0.0023	4.836	0.087	0.3127	0.0046	0.8821	0.1122	0.0010	1754	23	1835	16	4.4
7464-29.1	180	34	0.20	56	2	4.85E-05	1.87E-05	0.00084	0.0546	0.0012	4.775	0.079	0.3073	0.0043	0.9105	0.1127	0.0008	1728	21	1843	12	6.3
7464-22.1	227	48	0.22	67	2	2.65E-05	1.68E-05	0.00046	0.0603	0.0013	4.573	0.090	0.2940	0.0047	0.8671	0.1128	0.0011	1661	23	1845	18	10
7464-23.1	206	65	0.33	63	1	1.00E-05	1.00E-05	0.00017	0.0998	0.0024	4.552	0.126	0.2926	0.0073	0.9437	0.1128	0.0010	1655	36	1846	17	10.4
7464-14.1	130	34	0.27	42	0	1.00E-05	1.00E-05	0.00017	0.0807	0.0015	4.967	0.090	0.3185	0.0048	0.8882	0.1131	0.0010	1782	24	1850	15	3.7
7464-42.1	158	55	0.36	53	1	1.71E-05	2.71E-05	0.00030	0.1052	0.0025	4.954	0.097	0.3171	0.0054	0.9160	0.1133	0.0009	1775	26	1854	14	4.2
7464-54.1	117	36	0.32	39	6	1.78E-04	5.98E-05	0.00309	0.0879	0.0032	5.112	0.096	0.3248	0.0038	0.7182	0.1142	0.0015	1813	19	1867	24	2.9
7464-31.1	225	62	0.29	78	2	3.37E-05	3.74E-05	0.00030	0.1518	0.0024	5.087	0.081	0.3223	0.0045	0.8462	0.1143	0.0009	1867	19	1869	15	0.1
7464-17.1	216	111	0.53	76	2	2.07E-05	5.96E-05	0.00036	0.1091	0.0032	4.842	0.099	0.3067	0.0042	0.7545	0.1145	0.0016	1725	21	1872	25	7.9
7464-51.1	129	47	0.38	42	1	1.00E-05	1.00E-05	0.00017	0.0961	0.0017	4.840	0.080	0.3012	0.0043	0.9146	0.1166	0.0008	1697	31	1904	12	10.9
7464-52.1	227	73	0.33	71	1	1.36E-04	6.36E-05	0.00236	0.0928	0.0038	6.459	0.184	0.3767	0.0070	0.7357	0.1244	0.0024	2061	33	2020	35	-2
7464-7.1	62	45	0.75	27	3	2.28E-05	2.23E-05	0.00040	0.1463	0.0018	10.920	0.197	0.4714	0.0076	0.9350	0.1680	0.0011	2490	30	2538	11	1.9
7464-45.1	253	146	0.60	110	1	1.42E-05	1.42E-05	0.00025	0.1677	0.0015	7.899	0.121	0.3833	0.0054	0.9429	0.1483	0.0008	2092	25	2327	9	10.1
7464-55.1	92	64	0.72	46	3	8.46E-05	4.20E-05	0.00147	0.2072	0.0033	9.351	0.272	0.4270	0.0066	0.6290	0.1588	0.0036	2292	30	2443	39	6.2
7464-50.1	129	64	0.52	69	1	2.28E-05	2.23E-05	0.00040	0.1463	0.0018	10.920	0.197	0.4714	0.0076	0.9350	0.1680	0.0011	2490	30	2538	11	1.9
7464-39.1	216	63	0.30	109	1	1.00E-05	1.00E-05	0.00017	0.0825	0.0012	11.121	0.232	0.4692	0.0082	0.8914	0.1719	0.0016	2480	36	2576	16	3.7
7464-21.1	247	112	0.47	107	10	1.16E-04	3.58E-05	0.00201	0.1282	0.0025	9.277	0.195	0.3866	0.0074	0.9450	0.1740	0.0012	2107	34	2597	12	18.9
7464-2.1	208	88	0.44	108	2	2.56E-05	1.45E-05	0.00044	0.1214	0.0013	11.253	0.192	0.4687	0.0066	0.8860	0.1741	0.0014	2478	29	2598	13	4.6
7464-27.1	201	157	0.81	123	7	8.49E-05	3.19E-05	0.00147	0.2214	0.0024	12.550	0.209	0.5060	0.0074	0.9247	0.1799	0.0012	2639	32	2652	11	0.5
7464-24.1	179	90	0.52	103	0	2.47E-06	2.52E-05	0.00004	0.1460	0.0016	12.611	0.201	0.5019	0.0074	0.9550	0.1822	0.0009	2622	32	2673	8	1.9
7464-47.1	97	33	0.35	53	0	1.00E-05	1.00E-05	0.00017	0.0929	0.0046	12.567	0.222	0.4950	0.0076	0.9177	0.1841	0.0013	2592	33	2691	12	3.7
7464-41.1	231	91	0.41	117	1	1.00E-05	1.00E-05	0.00017	0.1085	0.0012	11.835	0.214	0.4509	0.0072	0.9343	0.1904	0.0012	2399	32	2745	11	12.6
7464-35.1	66	87	1.36	42	1	2.63E-05	2.66E-05	0.00046	0.3818	0.0054	13.141	0.279	0.4709	0.0081	0.8716	0.2024	0.0021	2487	36	2846	17	12.6
z7460 Wolverine Point Formation																						
7460-28.1	158	144	0.94	56	4	8.97E-05	4.01E-05	0.00156	0.2837	0.0081	4.255	0.073	0.2981	0.0039	0.8917	0.1035	0.0010	1682	19	1688	18	0.3
7460-28.1.2	154	141	0.94	54	6	1.45E-04	6.05E-05	0.00252	0.2797	0.0035	4.179	0.075	0.2952	0.0040	0.8286	0.1027	0.0010	1667	20	1673	19	0.3
7460-28.1.3	155	142	0.94	54	10	2.64E-04	4.51E-05	0.00457	0.2705	0.0063	4.077	0.080	0.2958	0.0039	0.7576	0.0999	0.0013	1671	19	1623	24	-2.9
7460-28.2	132	107	0.84	45	5	1.56E-04	3.87E-05	0.00270	0.2487	0.0027	4.181	0.075	0.2930	0.0042	0.8653	0.1035	0.0009	1657	21	1687	17	1.8
7460-28 mean																				1674	21	
7460-76.1	258	173	0.69	85	8	1.20E-04	2.68E-05	0.00208	0.1913	0.0021	4.140	0.062	0.2952	0.0037	0.8845	0.1017	0.0007	1667	18	1656	13	-0.7
7460-76.1.2																						

Table 2. (cont.)

Spot name	U (ppm)	Th (ppm)	Th/U	Pb* (ppm)	<sup>204</sup> Pb (ppb)	<sup>204</sup> Pb/ <sup>206</sup> Pb	<sup>204</sup> Pb/ <sup>206</sup> Pb	f(206) <sup>204</sup>	<sup>208</sup> Pb/ <sup>206</sup> Pb	<sup>208</sup> Pb/ <sup>206</sup> Pb	<sup>207</sup> Pb/ <sup>238</sup> U	<sup>207</sup> Pb/ <sup>238</sup> U	<sup>206</sup> Pb/ <sup>238</sup> U	<sup>206</sup> Pb/ <sup>238</sup> U	± <sup>206</sup> Pb/ <sup>238</sup> U	± <sup>206</sup> Pb/ <sup>238</sup> U	± <sup>207</sup> Pb/ <sup>238</sup> U	± <sup>207</sup> Pb/ <sup>238</sup> U	± <sup>206</sup> Pb/ <sup>238</sup> U	± <sup>206</sup> Pb/ <sup>238</sup> U	Apparent ages (Ma)				Disc. (%)
																					± <sup>206</sup> Pb/ <sup>238</sup> U	± <sup>206</sup> Pb/ <sup>238</sup> U	± <sup>207</sup> Pb/ <sup>238</sup> U	± <sup>207</sup> Pb/ <sup>238</sup> U	
7460-42.1	157	104	0.68	53	8	1.87E-04	8.42E-05	0.00324	0.1986	0.0039	4.179	0.088	0.2995	0.0040	0.7116	0.1012	0.0015	1689	20	1646	28	-2.6			
7460-42.1.2	153	104	0.70	51	7	1.67E-04	4.48E-05	0.00289	0.2100	0.0042	4.236	0.077	0.2973	0.0042	0.8356	0.1033	0.0010	1678	21	1685	19	0.4			
7460-42.1.3	162	114	0.73	52	7	1.82E-04	8.58E-05	0.00315	0.2172	0.0045	4.025	0.088	0.2818	0.0037	0.6906	0.1036	0.0017	1600	19	1690	30	5.3			
7460-42 mean	72	30	0.43	22	3	1.92E-04	8.08E-05	0.00333	0.1221	0.0047	4.124	0.100	0.2960	0.0048	0.7658	0.1046	0.0017	1621	24	1707	29	5.1			
7460-41.1	684	152	0.23	218	8	4.13E-05	8.14E-06	0.00072	0.0675	0.0006	4.632	0.107	0.3155	0.0038	0.6208	0.1065	0.0020	1768	19	1740	34	-1.6			
7460-5.1	197	61	0.32	63	4	7.71E-05	2.76E-05	0.00134	0.0922	0.0010	4.579	0.080	0.3070	0.0046	0.9157	0.1092	0.0008	1726	23	1769	13	2.4			
7460-20.1	425	84	0.20	139	4	3.62E-05	1.46E-05	0.00063	0.0604	0.0010	4.875	0.088	0.3252	0.0046	0.8482	0.1083	0.0011	1815	22	1771	18	-2.5			
7460-97.1	292	109	0.39	95	7	8.48E-05	2.05E-05	0.00147	0.1140	0.0023	4.649	0.075	0.3099	0.0044	0.8249	0.1088	0.0007	1740	22	1779	11	2.2			
7460-92.1	225	75	0.35	73	6	9.87E-05	2.42E-05	0.00171	0.0995	0.0020	4.699	0.090	0.3131	0.0046	0.9150	0.1088	0.0008	1756	23	1780	13	1.3			
7460-91.1	173	111	0.66	63	9	1.88E-04	3.90E-05	0.00326	0.1910	0.0033	4.928	0.090	0.3269	0.0049	0.8723	0.1093	0.0010	1823	24	1789	17	-1.9			
7460-70.1	396	106	0.33	106	7	8.29E-05	2.83E-05	0.00144	0.0972	0.0017	4.575	0.084	0.3024	0.0048	0.9182	0.1097	0.0008	1703	24	1795	13	5.1			
7460-44.1	140	62	0.46	49	5	1.22E-04	8.41E-05	0.00211	0.1333	0.0036	4.978	0.101	0.3287	0.0043	0.7286	0.1098	0.0016	1832	21	1797	26	-2			
7460-78.1	349	75	0.22	113	8	8.76E-05	2.69E-05	0.00152	0.0661	0.0026	4.840	0.101	0.3193	0.0055	0.8887	0.1099	0.0011	1786	27	1798	18	0.7			
7460-84.1	133	57	0.44	44	6	1.66E-04	6.49E-05	0.00287	0.1306	0.0037	4.736	0.113	0.3122	0.0050	0.7490	0.1100	0.0018	1752	24	1800	29	2.7			
7460-104.1	170	136	0.83	64	7	1.47E-04	3.15E-05	0.00255	0.2358	0.0034	4.888	0.084	0.3216	0.0047	0.8979	0.1102	0.0008	1798	23	1803	14	0.3			
7460-93.1	330	81	0.25	104	9	9.74E-05	2.72E-05	0.00169	0.0719	0.0017	4.765	0.083	0.3098	0.0048	0.9319	0.1116	0.0007	1740	24	1825	12	4.7			
7460-74.1	187	46	0.26	62	2	3.46E-05	2.41E-05	0.00060	0.0764	0.0021	5.032	0.122	0.3254	0.0060	0.8345	0.1122	0.0015	1816	29	1835	25	1			
7460-12.1	150	58	0.40	52	6	1.43E-04	5.03E-05	0.00247	0.1152	0.0026	5.034	0.096	0.3252	0.0049	0.8511	0.1123	0.0011	1815	24	1836	18	1.1			
7460-39.1	89	11	0.12	29	7	2.83E-04	5.92E-05	0.00490	0.0322	0.0025	5.203	0.123	0.3358	0.0064	0.8614	0.1124	0.0014	1866	31	1838	22	-1.5			
7460-89.1	229	34	0.15	75	10	1.54E-04	3.35E-05	0.00266	0.0425	0.0028	5.099	0.092	0.3287	0.0049	0.8774	0.1125	0.0010	1832	24	1841	16	0.5			
7460-17.1	239	356	1.54	105	9	1.29E-04	1.04E-04	0.00223	0.4373	0.0050	5.087	0.157	0.3277	0.0048	0.5811	0.1126	0.0029	1827	24	1842	47	0.8			
7460-52.1	201	106	0.55	72	8	1.45E-04	6.39E-05	0.00251	0.1556	0.0029	5.090	0.100	0.3277	0.0041	0.7238	0.1127	0.0015	1827	20	1843	25	0.8			
7460-87.1	119	47	0.38	41	5	1.43E-04	5.27E-05	0.00248	0.1112	0.0033	5.182	0.113	0.3329	0.0055	0.8230	0.1129	0.0014	1853	26	1846	23	-0.3			
7460-2.1	169	107	0.65	61	4	8.18E-05	2.77E-05	0.00142	0.1893	0.0030	5.007	0.098	0.3207	0.0048	0.8380	0.1132	0.0012	1793	24	1852	20	3.2			
7460-4.1	194	503	2.68	100	3	6.30E-05	3.38E-05	0.00109	0.7849	0.0052	4.947	0.087	0.3160	0.0047	0.9001	0.1136	0.0009	1770	23	1857	14	4.7			
7460-3.1	135	25	0.19	44	4	1.12E-04	3.43E-05	0.00193	0.0557	0.0018	5.099	0.100	0.3255	0.0052	0.8796	0.1136	0.0011	1816	26	1858	17	2.2			
7460-48.1	150	89	0.61	56	6	1.34E-04	3.83E-05	0.00233	0.1787	0.0024	5.276	0.101	0.3363	0.0049	0.8326	0.1138	0.0012	1899	24	1861	19	-0.5			
7460-21.1	151	80	0.20	52	4	9.62E-05	5.10E-05	0.00167	0.0650	0.0032	5.368	0.101	0.3416	0.0048	0.8149	0.1140	0.0013	1864	23	1864	20	-1.7			
7460-85.1	114	171	1.55	51	8	2.46E-04	4.89E-05	0.00426	0.4528	0.0078	5.211	0.143	0.3301	0.0063	0.7786	0.1145	0.0020	1839	31	1872	32	1.8			
7460-31.1	191	51	0.28	62	7	1.41E-04	8.00E-05	0.00245	0.0786	0.0032	5.026	0.103	0.3180	0.0044	0.7540	0.1146	0.0016	1780	22	1874	25	5			
7460-19.1	169	157	0.96	72	3	5.60E-05	2.68E-05	0.00097	0.2808	0.0035	5.986	0.104	0.3542	0.0053	0.9160	0.1225	0.0009	1955	25	1994	13	1.9			
7460-61.1	349	140	0.41	133	14	1.32E-04	1.08E-05	0.00228	0.1151	0.0019	6.068	0.103	0.3565	0.0053	0.9142	0.1234	0.0009	1966	25	2006	12	2			
7460-32.1	140	95	0.70	57	7	1.58E-04	5.17E-05	0.00273	0.2055	0.0055	6.088	0.261	0.3559	0.0061	0.5106	0.1241	0.0046	1963	29	2016	67	2.6			
7460-19.1	267	69	0.27	104	8	8.95E-05	1.89E-05	0.00155	0.0769	0.0012	6.577	0.102	0.3753	0.0048	0.8888	0.1271	0.0009	2054	23	2058	13	0.2			
7460-25.1	149	62	0.43	78	10	1.62E-04	4.47E-05	0.00281	0.1187	0.0024	10.421	0.188	0.4459	0.0068	0.8783	0.1465	0.0013	2377	30	2305	15	-3.1			
7460-30.1	168	61	0.37	81	7	1.14E-04	5.29E-05	0.00198	0.1062	0.0023	9.641	0.150	0.4402	0.0057	0.8857	0.1589	0.0012	2352	25	2444	12	3.8			
7460-43.1	158	62	0.41	85	6	9.66E-05	3.73E-05	0.00167	0.1170	0.0020	10.879	0.169	0.4876	0.0065	0.9084	0.1618	0.0011	2560	28	2475	11	-3.5			
7460-95.1	255	151	0.61	134	9	9.26E-05	1.56E-05	0.00160	0.1683	0.0021	10.301	0.158	0.4594	0.0066	0.9649	0.1626	0.0007	2437	29	2483	7	1.9			
7460-63.1	269	172	0.66	143	10	9.70E-05	1.82E-05	0.00168	0.1769	0.0017	10.368	0.140	0.4598	0.0056	0.9431	0.1635	0.0007	2439	25	2493	8	2.2			
7460-102.1	399	132	0.34	194	4	2.64E-05	8.38E-06	0.00046	0.0927	0.0013	10.189	0.151	0.4492	0.0061	0.9563	0.1645	0.0007	2392	27	2502	7	4.4			
7460-58.1	292	183	0.67	146	10	9.74E-05	2.00E-05	0.00169	0.1829	0.0018	10.270	0.174	0.4452	0.0069	0.9520	0.1673	0.0009	2374	31	2531	9	6.2			
7460-15.1	352	74	0.22	182	10	6.59E-05	2.66E-05	0.00114	0.0579	0.0012	11.348	0.152	0.4907	0.0059	0.9349	0.1677	0.0008	2574	25	2535	8	-1.5			
7460-40.1	311	105	0.35	162	6	4.87E-05	1.20E-05	0.00084	0.0972	0.0013	11.126	0.169	0.4728	0.0069	0.9730	0.1695	0.0006	2510	30	2553	6	1.7			
7460-40.1	227	87	0.40	118	5	5.89E-05	1.86E-05	0.00102	0.1099	0.0014	11.076	0.163	0.4728	0.0062	0.9396	0.1699	0.0009	2496	27	2557	9	2.4			
7460-57.1	219	119	0.56	122	14	1.54E-04	4.53E-05	0.00267	0.1518	0.0022	11.558	0.169	0.4886	0.0061	0.9020	0.1716	0.0011	2565	26	2573	11	0.3			
7460-18.1	671	284	0.44	366	7	2.38E-05	1.83E-05	0.00041	0.1226	0.0018	11.649	0.149	0.4996	0.0059	0.9676	0.1726	0.0006	2569	25	2583	5	0.5			
7460-26.1	348	184	0.55	193	4	2.85E-05	1.08E-05	0.00049	0.1538	0.0016	11.572	0.207	0.4858	0.0069	0.8572	0.1728	0.0016	2552	30	2585	16	1.3			
7460-56.1	435	312	0.74	260	13	7.01E-05	1.32E-05	0.00122	0.2040	0.0014	12.074	0.165	0.5039	0.0064	0.9608	0.1738	0.0007	2630	27	2595	6	-1.4			
7460-71.1	277	111	0.41	153	16	1.34E-04	2.75E-05	0.00235	0.1177	0.0021	11.978	0.178	0.4981	0.0063	0.9065	0.1744	0.0011	2606	27	2601	11	-0.2			
7460-10.1	74	40	0.56	39	4	1.24E-04	4.73E-05	0.00212	0.1560	0.0032	11.200	0.228	0.4651	0.0077	0.8754	0.1747	0.0017	2462	34	2603	17	5.4			



Table 2. (cont.)

Spot name	U (ppm)	Th (ppm)	Th/U	Pb* (ppm)	<sup>204</sup> Pb/ <sup>206</sup> Pb	<sup>204</sup> Pb/ <sup>206</sup> Pb	f(206) <sup>204</sup>	<sup>205</sup> Pb/ <sup>206</sup> Pb	<sup>205</sup> Pb/ <sup>206</sup> Pb	<sup>207</sup> Pb/ <sup>206</sup> Pb	<sup>207</sup> Pb/ <sup>206</sup> Pb	<sup>208</sup> Pb/ <sup>206</sup> Pb	<sup>208</sup> Pb/ <sup>206</sup> Pb	<sup>209</sup> Pb/ <sup>206</sup> Pb	<sup>209</sup> Pb/ <sup>206</sup> Pb	Apparent ages (Ma)				Disc. (%)	
																<sup>207</sup> Pb/ <sup>206</sup> Pb	<sup>207</sup> Pb/ <sup>206</sup> Pb	<sup>209</sup> Pb/ <sup>206</sup> Pb	<sup>209</sup> Pb/ <sup>206</sup> Pb		
7460-86.1	262	152	0.60	145	7	6.86E-05	1.73E-05	0.1690	0.0019	11.714	0.210	0.4789	0.0069	0.8622	0.1774	0.0016	2523	30	2629	15	4
7460-82.1	299	74	0.26	167	7	5.20E-05	1.49E-05	0.00090	0.0012	12.922	0.211	0.5185	0.0076	0.9375	0.1807	0.0016	2693	32	2660	10	-1.3
7460-35.1	292	75	0.33	129	6	6.24E-05	3.57E-05	0.00108	0.00934	12.618	0.189	0.5060	0.0067	0.9319	0.1809	0.0010	2640	29	2661	9	0.8
7460-14.1	168	293	1.80	127	6	8.33E-05	2.16E-05	0.00144	0.4859	13.111	0.200	0.5246	0.0071	0.9325	0.1812	0.0010	2719	30	2664	9	-2
7460-11.1	133	118	0.92	84	4	7.24E-05	3.60E-05	0.00125	0.2522	12.787	0.211	0.5069	0.0069	0.8893	0.1830	0.0014	2643	30	2680	13	1.4
7460-88.1	65	149	2.38	53	7	2.54E-04	6.03E-05	0.00440	0.6651	12.931	0.303	0.5107	0.0096	0.8643	0.1836	0.0022	2660	41	2686	20	1
7460-49.1	62	78	1.29	43	6	2.08E-04	4.36E-05	0.00361	0.3526	13.357	0.366	0.5263	0.0108	0.8194	0.1841	0.0029	2726	46	2690	26	-1.3
7460-47.1	112	49	0.45	64	7	1.50E-04	4.40E-05	0.00260	0.1263	12.991	0.243	0.5078	0.0081	0.9027	0.1856	0.0015	2647	35	2703	13	2.1
7460-79.1	157	338	2.23	124	9	1.29E-04	2.73E-05	0.00224	0.6210	13.059	0.255	0.5096	0.0078	0.8470	0.1859	0.0019	2655	33	2706	17	1.9
7460-9.1	198	185	0.96	129	3	3.81E-05	2.15E-05	0.00066	0.2659	13.346	0.229	0.5185	0.0078	0.9207	0.1867	0.0013	2693	33	2713	11	0.7
7460-34.1	483	168	0.36	315	6	2.60E-05	1.54E-05	0.00045	0.1003	15.805	0.325	0.5845	0.0111	0.9597	0.1961	0.0011	2967	45	2794	10	-6.2
7460-29.1	74	33	0.47	45	11	3.33E-04	1.20E-04	0.00577	0.1204	15.948	0.366	0.5354	0.0090	0.8097	0.2161	0.0029	2764	38	2952	22	6.4
7460-68.1	158	44	0.29	118	9	9.88E-05	2.02E-05	0.00171	0.0697	24.987	0.439	0.6434	0.0106	0.9675	0.2817	0.0013	3202	42	3372	7	5
z7462 Manitou Falls Formation, member D																					
7462-81.1	74	34	0.48	26	8	4.08E-04	9.54E-05	0.00707	0.1338	4.969	0.126	0.3273	0.0056	0.7526	0.1101	0.0019	1825	27	1801	31	-1.4
7462-81.2	81	42	0.53	28	3	1.40E-04	4.95E-05	0.00243	0.1615	4.824	0.095	0.3193	0.0048	0.8322	0.1096	0.0012	1786	23	1792	20	0.3
7462-81.3	73	38	0.54	21	0	1.77E-05	6.20E-05	0.00031	0.1594	4.086	0.094	0.2826	0.0043	0.7901	0.1129	0.0016	1503	22	1846	26	18.6
7462-81.1.2	75	34	0.47	27	6	2.66E-04	5.52E-05	0.00461	0.1379	5.075	0.136	0.3307	0.0057	0.7396	0.1113	0.0020	1842	28	1821	34	-1.1
7462-81.2.2	84	44	0.54	27	4	1.81E-04	4.38E-05	0.00313	0.1569	4.526	0.136	0.2945	0.0071	0.8661	0.1115	0.0017	1664	35	1823	28	8.8
7462-81 mean																					
7462-80.1	98	52	0.55	34	6	2.21E-04	4.75E-05	0.00383	0.1547	4.915	0.083	0.3181	0.0044	0.8689	0.1121	0.0010	1780	21	1833	15	2.9
7462-80.1.2	95	50	0.54	33	6	2.39E-04	4.17E-05	0.00414	0.1650	4.825	0.085	0.3188	0.0047	0.8943	0.1098	0.0009	1784	23	1796	14	0.7
7462-80.2	70	44	0.64	23	8	4.74E-04	8.94E-05	0.00822	0.1944	4.945	0.099	0.2954	0.0044	0.7641	0.1132	0.0016	1619	22	1852	26	12.6
7462-80 mean																					
7462-88.1	173	132	0.79	57	19	4.53E-04	9.56E-05	0.00784	0.2456	4.246	0.114	0.2794	0.0051	0.7660	0.1102	0.0019	1588	26	1803	32	11.9
7462-76.1	170	57	0.35	57	10	2.09E-04	4.11E-05	0.00362	0.0969	4.963	0.090	0.3240	0.0045	0.8419	0.1111	0.0011	1809	22	1817	18	0.4
7462-33.1	105	44	0.43	35	3	9.81E-05	5.51E-05	0.00170	0.1293	4.747	0.103	0.3095	0.0049	0.8016	0.1113	0.0015	1738	24	1820	24	4.5
7462-51.1	93	43	0.48	31	3	1.13E-04	4.13E-05	0.00196	0.1366	4.761	0.128	0.3104	0.0070	0.9001	0.1113	0.0013	1742	35	1820	22	4.3
7462-74.1	118	45	0.39	40	6	1.85E-04	7.71E-05	0.00320	0.1178	4.956	0.115	0.3225	0.0052	0.7803	0.1115	0.0016	1802	26	1824	27	1.2
7462-9.1	93	65	0.72	34	4	1.52E-04	4.08E-05	0.00264	0.2079	5.044	0.099	0.3281	0.0050	0.8409	0.1115	0.0012	1829	24	1824	20	-0.3
7462-61.1	146	80	0.57	53	2	5.86E-05	6.11E-05	0.00102	0.1678	5.082	0.099	0.3289	0.0048	0.8260	0.1117	0.0012	1833	24	1826	20	-0.4
7462-53.1	80	53	0.69	28	6	2.57E-04	7.35E-05	0.00445	0.1907	4.804	0.114	0.3119	0.0052	0.7779	0.1117	0.0017	1750	25	1827	27	4.2
7462-25.1	118	41	0.36	40	8	2.46E-04	4.79E-05	0.00427	0.1048	4.961	0.096	0.3218	0.0049	0.8508	0.1118	0.0012	1799	24	1829	19	1.6
7462-94.1	108	80	0.76	41	11	3.49E-04	8.87E-05	0.00605	0.2255	5.037	0.109	0.3265	0.0044	0.7094	0.1119	0.0017	1821	21	1830	28	0.5
7462-59.1	121	73	0.62	46	6	1.71E-04	6.93E-05	0.00297	0.1845	5.222	0.124	0.3383	0.0059	0.8118	0.1120	0.0016	1878	29	1831	25	-2.6
7462-93.1	87	67	0.79	32	2	9.34E-05	8.46E-05	0.00162	0.2418	4.911	0.101	0.3172	0.0044	0.7631	0.1123	0.0015	1776	22	1837	24	3.3
7462-95.1	134	44	0.34	45	7	1.88E-04	5.22E-05	0.00325	0.0991	4.973	0.091	0.3211	0.0045	0.8299	0.1123	0.0012	1795	22	1837	19	2.3
7462-39.1	114	52	0.47	39	6	1.92E-04	7.15E-05	0.00333	0.1366	4.976	0.107	0.3213	0.0050	0.8025	0.1123	0.0015	1796	25	1837	24	2.2
7462-89.1	93	58	0.64	34	8	3.13E-04	8.59E-05	0.00543	0.1858	5.106	0.120	0.3295	0.0049	0.7254	0.1124	0.0018	1836	24	1838	30	0.1
7462-52.1	91	53	0.60	32	4	1.48E-04	6.13E-05	0.00256	0.1795	4.844	0.104	0.3121	0.0049	0.8016	0.1126	0.0015	1751	24	1841	24	4.9
7462-38.1	75	59	0.54	25	3	1.32E-04	8.85E-05	0.00229	0.1590	4.865	0.132	0.3118	0.0059	0.7788	0.1132	0.0020	1750	29	1851	31	5.5
7462-113.1	223	38	0.17	74	4	6.44E-05	2.62E-05	0.00112	0.0524	5.236	0.089	0.3336	0.0043	0.8970	0.1139	0.0008	1856	21	1862	12	0.3
7462-73.1	158	95	0.62	57	6	1.46E-04	4.42E-05	0.00253	0.1804	5.120	0.089	0.3261	0.0044	0.8452	0.1139	0.0011	1819	22	1862	17	2.3
7462-96.1	150	93	0.64	55	5	1.21E-04	5.27E-05	0.00210	0.1865	5.119	0.108	0.3259	0.0055	0.8632	0.1139	0.0012	1819	27	1863	20	2.4
7462-28.1	159	120	0.78	59	11	2.64E-04	4.18E-05	0.00458	0.2420	4.983	0.102	0.3152	0.0063	0.9013	0.1147	0.0010	1766	27	1874	16	5.8
7462-18.1	40	19	0.50	14	2	2.05E-04	1.08E-04	0.00354	0.1499	5.228	0.158	0.3291	0.0063	0.7199	0.1152	0.0024	1834	31	1883	39	2.6
7462-46.1	117	67	0.59	44	10	3.05E-04	5.10E-05	0.00528	0.1734	5.342	0.119	0.3348	0.0062	0.8882	0.1157	0.0012	1862	30	1891	19	1.5
7462-96.1	125	75	0.62	46	8	2.27E-04	3.89E-05	0.00388	0.1780	5.366	0.090	0.3326	0.0046	0.8740	0.1170	0.0014	1851	22	1911	15	3.1
7462-27.1	76	32	0.43	28	6	2.76E-04	5.96E-05	0.00478	0.1248	5.621	0.117	0.3468	0.0054	0.8137	0.1176	0.0010	1919	26	1919	22	0
7462-54.1	160	96	0.62	59	3	7.07E-05	2.60E-05	0.00123	0.1785	5.342	0.105	0.3292	0.0052	0.8694	0.1177	0.0012	1834	25	1922	18	4.5
7462-24.1	142	69	0.50	53	0	1.00E-05	1.00E-05	0.00017	0.1479	5.579	0.112	0.3431	0.0056	0.8785	0.1179	0.0011	1901	27	1925	17	1.2
7462-110.1	112	137	1.27	47	6	1.83E-04	5.66E-05	0.00316	0.3889	5.319	0.098	0.3261	0.0049	0.8787	0.1183	0.0011	1819	24	1931	16	5.8

Table 2. (cont.)

Spot name	U (ppm)	Th (ppm)	Th/U	Pb* (ppm)	<sup>204</sup> Pb/ <sup>206</sup> Pb	<sup>204</sup> Pb/ <sup>206</sup> Pb	f(206) <sup>204</sup>	<sup>205</sup> Pb/ <sup>206</sup> Pb	<sup>205</sup> Pb/ <sup>206</sup> Pb	<sup>207</sup> Pb/ <sup>206</sup> Pb	<sup>207</sup> Pb/ <sup>206</sup> Pb	<sup>208</sup> Pb/ <sup>206</sup> Pb	<sup>208</sup> Pb/ <sup>206</sup> Pb	<sup>209</sup> Pb/ <sup>206</sup> Pb	<sup>209</sup> Pb/ <sup>206</sup> Pb	<sup>210</sup> Pb/ <sup>206</sup> Pb	<sup>210</sup> Pb/ <sup>206</sup> Pb	Apparent ages (Ma)		Disc. (%)		
																		<sup>207</sup> Pb/ <sup>206</sup> Pb	<sup>207</sup> Pb/ <sup>206</sup> Pb			
7462-13.1	124	73	0.61	45	3	8.22E-05	2.90E-05	0.00142	0.1804	0.0030	5.363	0.123	0.3284	0.0050	0.7469	0.1184	0.0018	1831	24	1933	28	5.3
7462-50.1	153	128	0.86	61	5	1.07E-04	3.28E-05	0.00185	0.2563	0.0025	5.510	0.094	0.3374	0.0048	0.8844	0.1184	0.0010	1874	23	1933	14	3
7462-65.1	191	94	0.51	72	3	4.71E-05	2.54E-05	0.00082	0.1519	0.0018	5.673	0.099	0.3461	0.0052	0.9083	0.1189	0.0009	1916	25	1940	13	1.2
7462-12.1	116	86	0.77	46	2	4.67E-05	3.44E-05	0.00081	0.2180	0.0031	5.768	0.100	0.3394	0.0065	0.8107	0.1232	0.0019	1884	31	2004	27	6
7462-56.1	159	61	0.39	60	3	6.82E-05	2.41E-05	0.00118	0.1158	0.0018	6.121	0.113	0.3522	0.0058	0.9367	0.1303	0.0008	1945	28	2044	12	4.8
7462-3.1	171	78	0.47	70	3	4.85E-05	4.54E-05	0.00084	0.1348	0.0030	6.726	0.120	0.3786	0.0055	0.8763	0.1289	0.0011	2070	26	2082	15	0.6
7462-6.1	43	69	1.68	22	3	2.50E-04	1.04E-04	0.00433	0.4877	0.0147	6.631	0.176	0.3690	0.0065	0.7464	0.1303	0.0023	2025	31	2102	32	3.7
7462-90.1	114	63	0.57	48	5	1.46E-04	3.39E-05	0.00253	0.1662	0.0028	6.748	0.113	0.3753	0.0064	0.9304	0.1304	0.0008	2054	26	2103	11	2.3
7462-14.1	68	75	1.13	36	11	4.48E-04	9.08E-05	0.00776	0.3278	0.0055	8.153	0.180	0.4110	0.0064	0.7864	0.1439	0.0020	2219	29	2275	24	2.4
7462-17.1	150	77	0.53	72	6	1.09E-04	2.86E-05	0.00189	0.1494	0.0020	8.750	0.176	0.4303	0.0077	0.9364	0.1475	0.0011	2307	35	2317	12	0.4
7462-34.1	128	62	0.50	60	7	1.42E-04	3.75E-05	0.00246	0.1392	0.0028	8.647	0.173	0.4232	0.0064	0.8282	0.1482	0.0017	2275	29	2325	20	2.2
7462-86.1	126	107	0.88	67	7	1.43E-04	4.30E-05	0.00248	0.2633	0.0041	9.074	0.181	0.4351	0.0068	0.8469	0.1513	0.0016	2329	31	2360	18	1.3
7462-30.1	183	88	0.50	95	10	1.32E-04	2.41E-05	0.00229	0.1383	0.0035	10.636	0.206	0.4598	0.0079	0.9329	0.1678	0.0012	2439	35	2535	12	3.8
7462-57.1	68	61	0.93	39	4	1.59E-04	4.32E-05	0.00275	0.2583	0.0039	10.912	0.180	0.4714	0.0069	0.9312	0.1679	0.0010	2490	30	2537	10	1.9
7462-101.1	87	54	0.65	49	6	1.55E-04	6.49E-05	0.00268	0.1801	0.0041	11.276	0.219	0.4859	0.0076	0.8660	0.1683	0.0017	2553	33	2541	16	-0.5
7462-47.1	144	72	0.51	79	3	4.84E-05	2.44E-05	0.00084	0.1451	0.0019	11.541	0.215	0.4854	0.0076	0.8916	0.1724	0.0015	2551	33	2581	14	1.2
7462-92.1	144	30	0.22	75	7	1.08E-04	2.79E-05	0.00187	0.0650	0.0015	11.898	0.209	0.4988	0.0077	0.9369	0.1762	0.0011	2570	33	2617	10	1.8
7462-111.1	31	22	0.75	19	7	4.99E-04	1.04E-04	0.00864	0.2031	0.0062	13.270	0.264	0.5086	0.0076	0.8270	0.1893	0.0021	2650	33	2736	19	3.1
7462-70.1	148	57	0.40	86	5	6.95E-05	2.42E-05	0.00120	0.1105	0.0015	13.610	0.219	0.5208	0.0077	0.9524	0.1896	0.0009	2702	33	2738	8	1.3
7462-22.1	73	6	0.09	36	12	4.05E-04	6.72E-05	0.00702	0.0197	0.0027	12.887	0.244	0.4666	0.0072	0.8765	0.2003	0.0018	2468	32	2829	15	12.7
7462-15.1	69	22	0.33	32	12	5.02E-04	7.74E-05	0.00871	0.1076	0.0036	11.739	0.255	0.4171	0.0070	0.8437	0.2041	0.0024	2247	32	2860	19	21.4
7462-32.1	135	90	0.69	84	14	2.32E-04	3.97E-05	0.00402	0.2081	0.0025	15.313	0.289	0.5032	0.0082	0.9131	0.2207	0.0017	2627	35	2986	13	12
z7465 Manitou Falls Formation, member B																						
7465-20.1	117	136	1.201	48	3	1.01E-04	4.11E-05	0.00175	0.3553	0.0051	4.940	0.111	0.3260	0.0062	0.8941	0.1089	0.0011	1819	30	1798	19	-1.2
7465-20.1.2	144	134	1.2074	47	4	1.27E-04	3.78E-05	0.00220	0.3481	0.0073	4.991	0.105	0.3252	0.0055	0.8732	0.1113	0.0012	1815	27	1821	19	0.3
7465-20.2	168	184	1.1266	60	6	1.50E-04	3.52E-05	0.00260	0.3242	0.0047	4.483	0.101	0.2894	0.0055	0.8999	0.1124	0.0011	1638	28	1838	18	10.9
7465-20 mean																						
7465-32.1	134	130	1.00	51	3	7.03E-05	2.43E-05	0.00122	0.2910	0.0030	4.824	0.086	0.3161	0.0047	0.8901	0.1107	0.0009	1771	23	1811	15	2.2
7465-32.2	134	131	1.00	52	3	6.80E-05	3.28E-05	0.00118	0.2944	0.0032	4.927	0.098	0.3204	0.0053	0.8902	0.1115	0.0010	1792	26	1825	17	1.8
7465-32.3	163	156	0.99	64	0	1.00E-05	1.00E-05	0.00017	0.2895	0.0030	5.048	0.110	0.3242	0.0058	0.8775	0.1129	0.0012	1810	28	1847	19	2
7465-32.4	146	137	0.97	46	2	4.81E-05	5.19E-05	0.00083	0.2791	0.0109	3.983	0.136	0.2610	0.0076	0.9063	0.1107	0.0016	1495	39	1810	27	17.4
7465-32 mean																						
7465-18.1	40	38	0.9693	15	7	6.44E-04	1.33E-04	0.01117	0.2588	0.0129	4.631	0.143	0.3133	0.0055	0.6609	0.1072	0.0025	1757	27	1753	43	-0.2
7465-18.2	48	59	1.2809	20	3	2.60E-04	8.21E-05	0.00450	0.3744	0.0069	5.160	0.112	0.3250	0.0050	0.7824	0.1151	0.0016	1814	24	1882	25	3.6
7465-18.3	38	43	1.1853	15	3	3.31E-04	9.23E-05	0.00573	0.3443	0.0084	5.011	0.114	0.3161	0.0049	0.7611	0.1150	0.0017	1771	24	1880	27	5.8
7465-18.4	49	51	1.0731	18	6	4.81E-04	1.08E-04	0.00833	0.2981	0.0077	4.845	0.136	0.3072	0.0048	0.6468	0.1144	0.0025	1727	23	1870	39	7.7
7465-8.1	82	104	1.32	35	5	2.14E-04	9.87E-05	0.00371	0.3894	0.0100	5.106	0.120	0.3335	0.0044	0.6551	0.1110	0.0020	1855	21	1816	33	-2.1
7465-8.1.2	77	96	1.2827	33	6	2.52E-04	6.70E-05	0.00436	0.3745	0.0054	5.065	0.120	0.3293	0.0054	0.7643	0.1116	0.0017	1835	26	1825	28	-0.6
7465-74.1	184	73	0.4109	63	5	1.05E-04	3.05E-05	0.00183	0.1188	0.0022	4.927	0.080	0.3224	0.0044	0.9028	0.1109	0.0008	1801	22	1813	13	0.7
7465-2.1	162	130	0.83	60	2	4.67E-05	2.94E-05	0.00081	0.2400	0.0039	4.856	0.127	0.3166	0.0057	0.7652	0.1112	0.0019	1773	28	1820	31	2.6
7465-29.1	80	71	0.91	31	2	8.76E-05	6.81E-05	0.00152	0.2629	0.0043	5.016	0.112	0.3270	0.0051	0.7785	0.1112	0.0016	1824	25	1820	26	-0.2
7465-42.1	174	49	0.29	57	0	1.00E-05	1.00E-05	0.00017	0.0838	0.0013	4.914	0.080	0.3200	0.0045	0.9185	0.1114	0.0010	1790	22	1822	12	1.8
7465-39.1	89	124	1.4459	36	6	2.44E-04	6.16E-05	0.00422	0.4147	0.0071	4.762	0.097	0.3089	0.0046	0.8081	0.1114	0.0013	1740	23	1822	22	4.5
7465-39.2	79	106	1.3838	29	6	2.87E-04	6.90E-05	0.00497	0.3999	0.0083	4.324	0.114	0.2813	0.0056	0.8205	0.1115	0.0017	1598	28	1824	28	12.4
7465-25.1	77	96	1.2918	32	5	2.28E-04	7.42E-05	0.00395	0.3761	0.0064	4.983	0.108	0.3241	0.0056	0.7823	0.1115	0.0015	1810	24	1824	25	0.8
7465-78.1	87	80	0.94	33	5	2.18E-04	1.18E-04	0.00378	0.2703	0.0058	4.926	0.140	0.3199	0.0056	0.7097	0.1117	0.0023	1789	28	1827	37	2
7465-12.1	73	89	1.27	29	2	8.63E-05	4.20E-05	0.00150	0.3671	0.0058	4.905	0.109	0.3177	0.0047	0.7519	0.1120	0.0017	1779	23	1832	27	2.9
7465-11.1	204	89	0.45	70	3	6.02E-05	4.15E-05	0.00104	0.1292	0.0022	4.956	0.097	0.3209	0.0050	0.8601	0.1120	0.0011	1794	24	1832	18	2.1
7465-61.1	151	214	1.46	63	6	1.37E-04	4.01E-05	0.00238	0.4330	0.0043	4.811	0.086	0.3113	0.0041	0.8055	0.1121	0.0012	1747	20	1834	20	4.7
7465-50.1	253	75	0.30	84	1	1.01E-05	2.16E-05	0.00017	0.0923	0.0015	4.957	0.078	0.3199	0.0044	0.8260	0.1124	0.0007	1789	22	1838	11	2.7
7465-69.1	148	53	0.37	50	1	2.09E-05	3.71E-05	0.00036	0.1105	0.0021	4.941	0.086	0.3187	0.0045	0.8819	0.1124	0.0009	1784	22	1839	15	3
7465-33.1	152	206	1.40	66	3	5.89E-05	2.49E-05	0.00102	0.4000	0.0039	5.157	0.125	0.3324	0.0072	0.9391	0.1125	0.0010	1850	35	1841	15	-0.5





Table 2. (cont.)

Spot name	U (ppm)	Th (ppm)	Th/U	Pb* (ppm)	<sup>204</sup> Pb/ <sup>200</sup> Pb (ppb)	$\pm \frac{204}{200}\text{Pb}$	$\pm \frac{204}{200}\text{Pb}$	f(206) <sup>204</sup>	$\frac{205}{206}\text{Pb}$	$\pm \frac{205}{206}\text{Pb}$	$\frac{207}{205}\text{Pb}$	$\pm \frac{207}{205}\text{Pb}$	$\frac{206}{208}\text{Pb}$	$\pm \frac{206}{208}\text{Pb}$	Corr. coeff.	$\frac{207}{206}\text{Pb}$	$\pm \frac{207}{206}\text{Pb}$	Apparent ages (Ma)				Disc. (%)
																		$\frac{206}{208}\text{Pb}$	$\pm \frac{206}{208}\text{Pb}$	$\frac{206}{208}\text{Pb}$	$\pm \frac{206}{208}\text{Pb}$	
7461-20.1	77	79	1.05	32	6	2.85E-04	7.74E-05	0.00493	0.2958	0.0058	5.431	0.147	0.3421	0.0057	0.7034	0.1151	0.0022	1897	27	1882	35	-0.8
7461-20.2	76	78	1.07	30	6	2.59E-04	8.28E-05	0.00448	0.2906	0.0078	5.027	0.126	0.3267	0.0058	0.7915	0.1116	0.0017	1823	28	1826	28	0.2
7461-20.3	83	77	0.95	33	0	2.12E-05	8.47E-05	0.00037	0.2795	0.0049	5.322	0.128	0.3248	0.0054	0.7676	0.1189	0.0019	1813	26	1939	28	6.5
7461-81.1	627	138	0.23	211	6	3.33E-05	9.83E-06	0.00058	0.0683	0.0010	5.284	0.069	0.3312	0.0040	0.9641	0.1157	0.0004	1844	19	1891	6	2.5
7461-13.1	117	85	0.75	46	4	1.11E-04	4.66E-05	0.00192	0.2140	0.0055	5.516	0.200	0.3457	0.0085	0.7579	0.1157	0.0028	1914	41	1891	44	-1.2
7461-27.1	325	36	0.11	105	4	3.92E-05	1.58E-05	0.00068	0.0313	0.0011	5.244	0.081	0.3286	0.0041	0.8746	0.1158	0.0009	1832	20	1892	14	3.2
7461-48.1	744	226	0.31	258	6	2.92E-05	6.33E-06	0.00051	0.0919	0.0011	5.337	0.077	0.3341	0.0046	0.9776	0.1159	0.0004	1858	22	1893	5	1.9
7461-26.1	137	217	1.63	63	2	4.33E-05	7.52E-05	0.00075	0.4725	0.0059	5.415	0.114	0.3379	0.0043	0.6975	0.1162	0.0018	1876	21	1899	28	1.2
7461-100.1	395	256	0.67	157	8	6.45E-05	1.62E-05	0.00112	0.1929	0.0027	5.684	0.078	0.3538	0.0042	0.9194	0.1165	0.0006	1953	20	1903	10	-2.6
7461-66.1	235	378	1.66	111	9	1.26E-04	2.94E-05	0.00218	0.4811	0.0054	5.496	0.127	0.3419	0.0050	0.7203	0.1166	0.0019	1896	24	1905	29	0.5
7461-16.1	459	243	0.55	177	7	4.98E-05	1.34E-05	0.00086	0.1556	0.0012	5.668	0.078	0.3517	0.0040	0.8775	0.1169	0.0008	1943	19	1909	12	-1.8
7461-10.1	221	135	0.63	84	4	6.82E-05	3.59E-05	0.00118	0.1812	0.0038	5.471	0.161	0.3393	0.0069	0.7742	0.1169	0.0022	1883	33	1910	34	1.4
7461-14.1	204	285	1.44	96	2	3.93E-05	3.21E-05	0.00068	0.4173	0.0033	5.734	0.094	0.3537	0.0045	0.8428	0.1176	0.0010	1952	21	1920	16	-1.7
7461-91.1	409	132	0.33	151	5	3.99E-05	1.27E-05	0.00069	0.0969	0.0011	5.725	0.091	0.3525	0.0045	0.9417	0.1178	0.0006	1946	21	1923	9	-1.2
7461-24.1.1	166	237	1.47	75	3	6.33E-05	3.50E-05	0.00110	0.4261	0.0046	5.508	0.096	0.3390	0.0042	0.7848	0.1178	0.0013	1882	20	1924	20	2.2
7461-53.1	159	70	0.45	59	2	3.63E-05	9.65E-05	0.00063	0.1306	0.0040	5.603	0.117	0.3448	0.0043	0.6878	0.1179	0.0018	1910	21	1924	28	0.8
7461-65.1	338	196	0.60	129	4	4.48E-05	2.26E-05	0.00078	0.1762	0.0023	5.609	0.088	0.3415	0.0048	0.9330	0.1191	0.0007	1894	23	1943	10	2.5
7461-15.1	658	45	0.07	233	1	1.00E-05	6.61E-06	0.00017	0.0196	0.0004	6.115	0.151	0.3602	0.0048	0.6412	0.1231	0.0024	1983	23	2002	34	1
7461-59.1	77	29	0.39	30	2	6.66E-05	4.27E-05	0.00115	0.1126	0.0054	6.558	0.152	0.3647	0.0062	0.8082	0.1304	0.0018	2005	29	2103	24	4.7
7461-71.1	87	73	0.86	38	2	8.22E-05	4.14E-05	0.00142	0.2437	0.0082	6.826	0.135	0.3707	0.0062	0.8972	0.1336	0.0012	2033	29	2145	16	5.3
7461-74.1	156	140	0.93	86	4	6.31E-05	2.83E-05	0.00109	0.2685	0.0048	9.382	0.167	0.4529	0.0058	0.7992	0.1503	0.0016	2408	26	2349	19	-2.5
7461-80.1	272	95	0.36	122	5	5.59E-05	1.61E-05	0.00097	0.1035	0.0012	8.689	0.135	0.4160	0.0054	0.8890	0.1515	0.0011	2242	24	2363	12	5.1
7461-86.1	363	68	0.19	166	4	2.95E-05	9.69E-06	0.00051	0.0563	0.0007	9.433	0.124	0.4385	0.0053	0.9586	0.1560	0.0006	2344	24	2413	6	2.9
7461-49.1	214	16	0.08	96	1	1.00E-05	1.00E-05	0.00017	0.0280	0.0013	9.544	0.167	0.4424	0.0066	0.8996	0.1565	0.0012	2361	29	2418	13	2.3
7461-42.1	300	62	0.21	144	5	3.92E-05	1.15E-05	0.00068	0.0582	0.0011	10.149	0.174	0.4569	0.0065	0.8836	0.1611	0.0013	2426	29	2467	14	1.7
7461-29.1	162	56	0.36	76	3	5.22E-05	3.71E-05	0.00090	0.1029	0.0019	9.518	0.189	0.4278	0.0057	0.7498	0.1614	0.0021	2436	26	2470	23	7.1
7461-94.1	180	74	0.43	91	9	1.31E-04	4.10E-05	0.00226	0.1223	0.0023	10.513	0.171	0.4591	0.0060	0.8652	0.1661	0.0021	2496	27	2519	14	3.3
7461-45.1	158	61	0.40	77	13	2.11E-04	3.22E-05	0.00365	0.1150	0.0022	10.110	0.175	0.4412	0.0068	0.9391	0.1662	0.0010	2356	31	2520	10	6.5
7461-77.1	257	110	0.44	134	7	7.10E-05	1.54E-05	0.00123	0.1220	0.0013	10.793	0.158	0.4705	0.0064	0.9585	0.1664	0.0007	2486	28	2522	7	1.4
7461-44.1	88	39	0.45	46	3	8.43E-05	2.87E-05	0.00146	0.1264	0.0027	10.895	0.204	0.4680	0.0076	0.9158	0.1688	0.0013	2475	33	2546	13	2.8
7461-57.1	131	48	0.38	67	1	2.07E-05	2.12E-05	0.00036	0.1105	0.0017	10.831	0.205	0.4666	0.0060	0.6984	0.1691	0.0029	2465	30	2548	29	3.3
7461-85.1	130	245	1.94	94	7	1.24E-04	2.84E-05	0.00214	0.5392	0.0046	11.363	0.214	0.4871	0.0064	0.7802	0.1692	0.0020	2558	28	2550	20	-0.3
7461-68.1	31	5	0.18	16	3	2.11E-04	1.48E-04	0.00365	0.0579	0.0064	11.388	0.322	0.4876	0.0098	0.7912	0.1694	0.0030	2560	43	2552	29	-0.3
7461-25.1	156	52	0.34	79	4	5.68E-05	6.67E-05	0.00098	0.0961	0.0031	10.931	0.205	0.4666	0.0060	0.7691	0.1699	0.0021	2469	27	2557	20	3.4
7461-95.1	79	71	0.93	44	3	1.00E-04	5.17E-05	0.00174	0.2591	0.0043	10.648	0.202	0.4506	0.0071	0.8911	0.1714	0.0015	2398	32	2571	15	6.8
7461-60.1	409	84	0.21	213	3	1.65E-05	5.89E-06	0.00029	0.0584	0.0007	11.687	0.169	0.4933	0.0058	0.8689	0.1718	0.0012	2585	25	2576	12	-0.4
7461-69.1	719	160	0.23	373	1	4.72E-06	5.65E-06	0.00008	0.0659	0.0039	11.554	0.171	0.4874	0.0067	0.9585	0.1719	0.0007	2559	29	2576	7	0.7
7461-7.1	406	292	0.74	228	2	1.39E-05	7.17E-06	0.00024	0.2079	0.0022	11.261	0.235	0.4736	0.0081	0.8820	0.1725	0.0017	2499	36	2582	17	3.2
7461-47.1	189	61	0.33	100	1	1.36E-05	1.50E-05	0.00024	0.0947	0.0017	11.528	0.192	0.4840	0.0072	0.9348	0.1728	0.0010	2545	31	2585	10	1.5
7461-1.1	226	90	0.41	122	3	3.35E-05	1.39E-05	0.00058	0.1116	0.0028	11.685	0.209	0.4904	0.0061	0.7696	0.1728	0.0020	2572	26	2585	19	0.5
7461-102.1	453	130	0.30	229	11	6.01E-05	1.20E-05	0.00104	0.0764	0.0009	11.959	0.159	0.4708	0.0059	0.9341	0.1731	0.0009	2487	26	2588	9	3.9
7461-30.1	235	112	0.49	122	3	3.12E-05	1.38E-05	0.00054	0.1390	0.0024	10.977	0.150	0.4599	0.0053	0.8938	0.1731	0.0011	2439	23	2588	10	5.8
7461-51.1	166	64	0.40	91	4	5.13E-05	2.05E-05	0.00089	0.1123	0.0015	11.911	0.188	0.4847	0.0059	0.8284	0.1746	0.0016	2591	26	2603	15	0.4
7461-31.1	577	388	0.69	327	3	1.40E-05	8.14E-06	0.00024	0.1911	0.0013	11.604	0.160	0.4812	0.0059	0.8747	0.1749	0.0012	2533	24	2605	11	2.8
7461-92.1	273	93	0.35	150	7	6.27E-05	1.42E-05	0.00109	0.0995	0.0013	12.134	0.191	0.5017	0.0073	0.9543	0.1754	0.0008	2621	31	2610	8	-0.4
7461-12.1	457	160	0.36	249	3	1.36E-05	8.22E-06	0.00024	0.0997	0.0008	12.028	0.166	0.4972	0.0063	0.9580	0.1755	0.0007	2602	27	2610	7	0.3
7461-9.1	357	261	0.76	209	2	1.37E-05	5.92E-06	0.00024	0.2068	0.0046	11.927	0.157	0.4922	0.0057	0.9158	0.1758	0.0009	2580	24	2613	9	1.3
7461-17.1	461	216	0.48	266	3	1.56E-05	8.23E-06	0.00027	0.1352	0.0010	12.450	0.171	0.5121	0.0060	0.9119	0.1763	0.0010	2665	26	2619	9	-1.8
7461-5.1	129	59	0.48	74	5	8.93E-05	3.30E-05	0.00155	0.1391	0.0023	12.241	0.194	0.5034	0.0131	0.7303	0.1764	0.0049	2628	56	2619	47	-0.4
7461-108.1	211	67	0.33	115	8	8.50E-05	1.99E-05	0.00147	0.0891	0.0013	12.140	0.217	0.4992	0.0069	0.8404	0.1764	0.0017	2610	30	2619	16	0.3
7461-21.1	449	289	0.67</																			



**Table 2. (cont.)**

Spot name	U (ppm)	Th (ppm)	Th/U	Pb* (ppm)	<sup>204</sup> Pb (ppb)	<sup>204</sup> Pb/ <sup>206</sup> Pb	$\pm \frac{204}{206} \text{Pb}$	$\pm \frac{204}{206} \text{Pb}$	$\frac{206}{206} \text{Pb}$	$\frac{207}{206} \text{Pb}$	$\pm \frac{207}{206} \text{Pb}$	$\frac{207}{206} \text{Pb}$	$\pm \frac{207}{206} \text{Pb}$	Apparent ages (Ma)			Disc. (%)					
														$\frac{206}{238} \text{U}$	$\frac{206}{238} \text{U}$	$\frac{206}{238} \text{U}$		$\frac{206}{238} \text{U}$	$\frac{207}{238} \text{U}$	$\frac{207}{238} \text{U}$	$\frac{207}{238} \text{U}$	
7461-56.1	243	172	0.73	148	2	1.84E-05	1.36E-05	0.00032	0.2050	0.0017	12.835	0.180	0.5104	0.0061	0.9070	0.1824	0.0011	2658	26	2675	10	0.6
7461-35.1	143	143	1.03	95	3	5.06E-05	1.71E-05	0.00088	0.2826	0.0051	13.467	0.340	0.5238	0.0096	0.7977	0.1865	0.0029	2715	41	2711	26	-0.1
7461-103.1	97	34	0.36	55	4	1.01E-04	7.51E-05	0.00175	0.1010	0.0034	13.265	0.304	0.5116	0.0096	0.8781	0.1880	0.0021	2664	41	2725	18	2.3
7461-8.1	103	73	0.73	63	3	7.65E-05	5.54E-05	0.00133	0.2039	0.0042	13.502	0.278	0.5107	0.0084	0.8606	0.1918	0.0020	2659	36	2757	17	3.6
7461-34.1	270	73	0.28	163	6	4.85E-05	2.49E-05	0.00084	0.0774	0.0013	15.114	0.193	0.5485	0.0061	0.9190	0.1999	0.0010	2819	25	2825	8	0.2
7461-106.1	96	88	0.95	67	4	9.08E-05	5.79E-05	0.00157	0.0036	0.0036	16.277	0.261	0.5539	0.0073	0.8821	0.2131	0.0016	2842	30	2929	12	3
7461-19.1	55	35	0.65	39	3	9.46E-05	6.16E-05	0.00164	0.1774	0.0043	17.773	0.474	0.5809	0.0117	0.8262	0.2219	0.0034	2953	48	2994	25	1.4
7461-93.1	430	144	0.35	317	5	2.00E-05	1.28E-05	0.00035	0.0917	0.0009	23.081	0.293	0.6315	0.0077	0.9802	0.2651	0.0007	3155	30	3277	4	3.7

Notes (see Stern, 1997):  
 \* = corrected for common Pb  
 Corr. coeff. = correlation coefficient  
 Disc. = discordance  
 Uncertainties are reported at 1  $\sigma$  (absolute) and are calculated by numerical propagation of all known sources of error.  
 $f(206)^{204}$  refers to mole fraction of total <sup>206</sup>Pb that is due to common Pb, calculated using the <sup>204</sup>Pb method; common-Pb composition used is the surface blank.  
 Discordance relative to origin =  $100 \cdot (1 - \frac{^{206}\text{Pb}/^{238}\text{U}}{^{206}\text{Pb}/^{238}\text{U}})$   
 Groups of replicate analyses are shaded in grey.  
 Spots labelled xxxx-y.z refer to replicate spots placed in a pre-existing SHRIMP pit. The U-Pb fractionation behaviour from these deeper pits varies from the values used in the U-Pb calibration. As such only Pb/Pb ages are considered accurate from these types of replicate analyses.

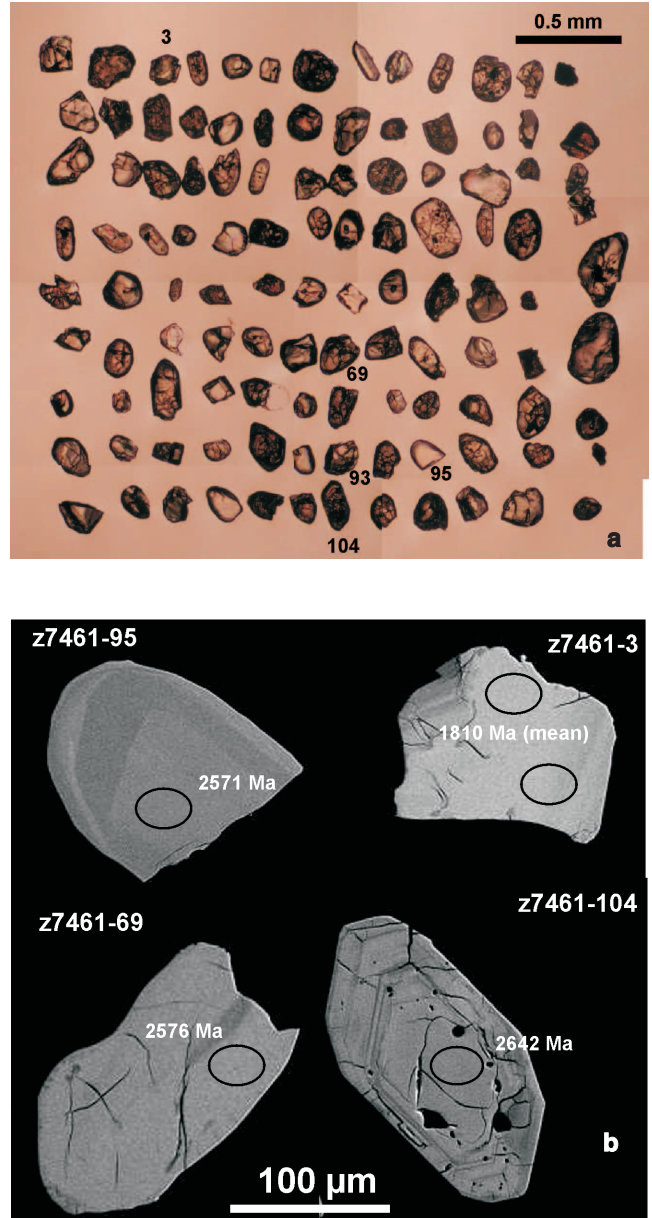


**Figure 4. a)** Transmitted-light image of the sample of detrital zircons picked from the Fair Point Formation (z7461). Numbers in figure refer to the grain-identification numbers used during SHRIMP analysis and mentioned in the text. **b)** Back-scattered-electron images of a representative selection of zircon grains. Ellipses represent approximate positions of SHRIMP analysis. Spot <sup>207</sup>Pb/<sup>206</sup>Pb ages are reported; see Table 2 for more details.

histogram (bin width = 25 Ma). Ages range from 1810 Ma to 3277 Ma, and all results are discordant by less than 10%. The most prominent age modes are 1900 Ma ( $n \approx 14$ ), 2520 Ma ( $n \approx 6$ ), 2585 Ma ( $n \approx 7$ ), and 2610 Ma ( $n \approx 9$ ). One younger grain was identified (grain 3, Fig. 4). Five replicate analyses of this grain produced a weighted mean  $^{207}\text{Pb}/^{206}\text{Pb}$  age of  $1810 \pm 15$  Ma (95% confidence),  $\text{MSWD} = 2.0$ , probability of fit = 9%. This age constrains the maximum timing of deposition for the Fair Point Formation and the Athabasca Group. Specific age modes are not clearly correlatable with zircon morphology. Generally, the more angular fragments give the younger ages (ca. 1900 Ma); however, there are a significant number of exceptions (i.e. young, rounded grains or old, fragmental grains). For example, the oldest grain (grain 93, 3277 Ma) is fairly angular (Fig. 4).

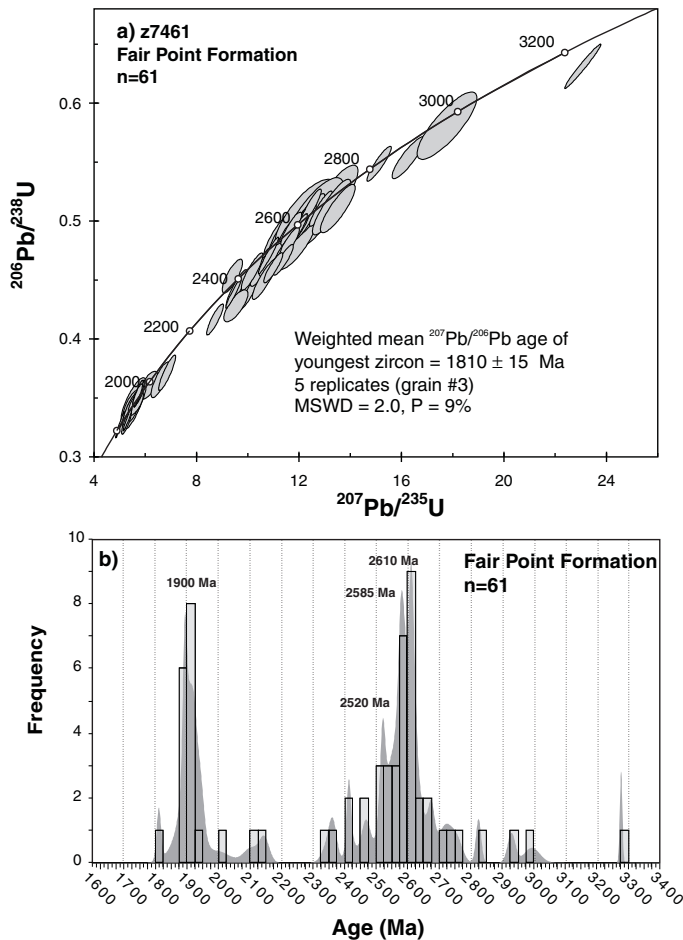


**Figure 5. a)** Concordia diagram of U-Pb results from sample z7461. Replicate analyses were not plotted. Error ellipses are at  $2\sigma$ . **b)** Cumulative probability curve with overlain histogram. Bin width is 25 Ma, yielding 55% efficiency (Sircombe, 2000). Replicate analyses are not included.

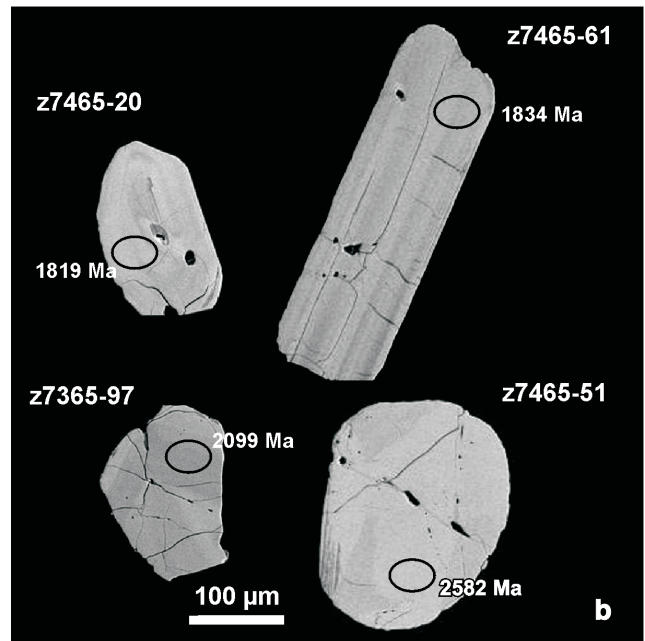


**Figure 6. a)** Transmitted-light image of the sample of detrital zircons picked from z7465 (Manitou Falls Formation, member B). Numbers in figure refer to the grain-identification numbers used during SHRIMP analysis and mentioned in the text. **b)** Backscattered-electron images of a representative selection of zircon grains. Ellipses represent approximate positions of SHRIMP analysis. Spot  $^{207}\text{Pb}/^{206}\text{Pb}$  ages are reported; see Table 2 for more details.

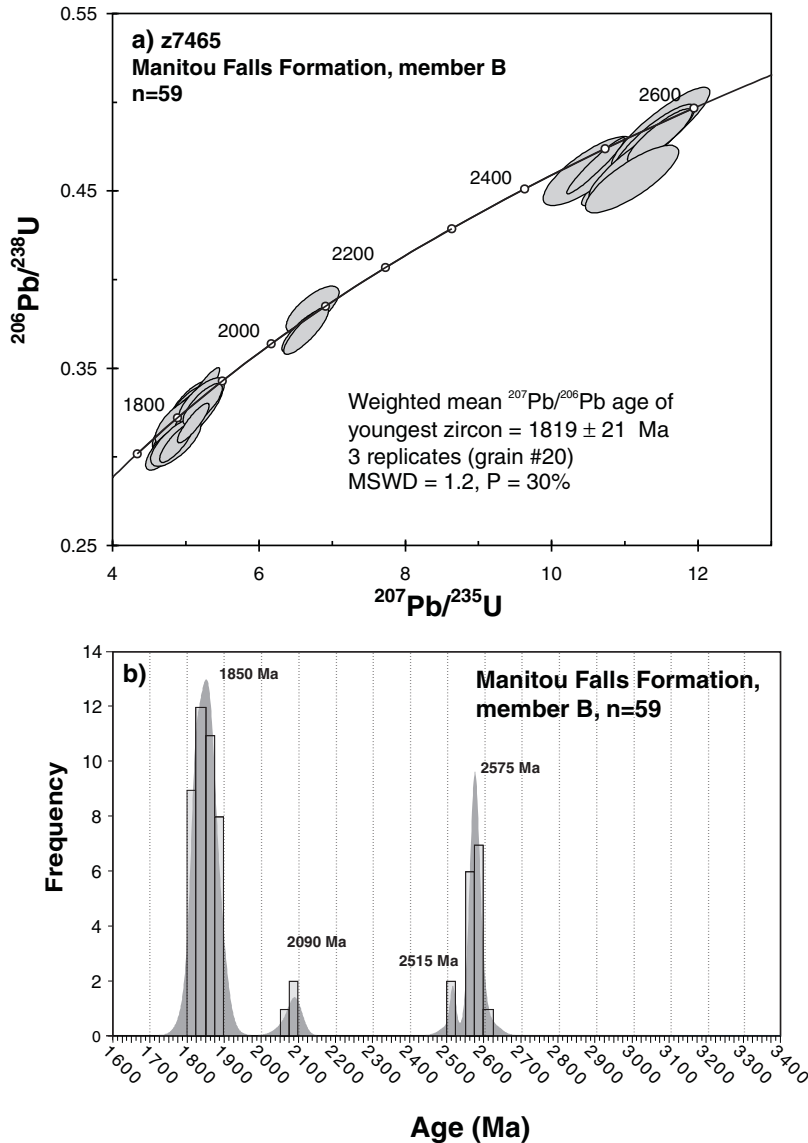


**Figure 7.**

*a) Concordia diagram of U-Pb results from sample z7465. Analyses discordant by >10% and replicate analyses were not plotted. Error ellipses are at  $2\sigma$ . b) Cumulative probability curve with overlain histogram. Bin width is 25 Ma, yielding 50% efficiency (Sircombe, 2000). Analyses discordant by >10% and replicate analyses were not included.*

### **Z7465 Manitou Falls Formation, member B**

A sample of the detrital zircon population from z7465 is shown in Figure 6. The dominant zircon morphology consists of excellent- to moderate-quality, colourless to pale brown, elongate tabular prisms. Facets are sharp to subrounded, and the grains range from slightly to highly fractured. In BSE images, typical zircons display faint concentric zoning (*see* Fig. 6, grain 20) or straight zoning (*see* Fig. 6, grain 61). Other morphologies observed include colourless, angular, anhedral fragments with faint, weakly concentric zoning or no zoning (*see* Fig. 6, grain 97). Well rounded, elongate to equant grains are also present. These grains generally are unzoned; a few exhibit faint concentric zoning in BSE (*see* Fig. 6, grain 51). The final zircon type is mainly distinguished by its pink-orange colour. These zircons have subrounded, blocky, and fragmental form and in BSE images are unzoned to weakly concentrically zoned (*see* Fig. 6, grains 23, 24, 27, 37).

The results for sample z7465 are illustrated on a concordia diagram and cumulative probability curve with overlain histogram (bin width = 25 Ma) in Figure 7. A total of 72 analyses were carried out on 62 different detrital zircon grains. The individual analyses form a largely bimodal distribution with the majority of the grains ( $n=42$ ) yielding ages ranging from 1819 to 1900 Ma. These form a roughly Gaussian distribution centred at 1850 Ma (Fig. 7b). Zircons within this age range typically have prismatic or fragmental morphologies. The second prominent mode, centred at 2575 Ma, groups 15 grains ranging in age from 2557 to 2619 Ma. The more rounded zircon grains generally yield this older age. A few analyses also yield ages of ca. 2090 Ma and 2515 Ma. Although not resolvable on the cumulative probability curve, there exists a younger age mode within the ca. 1850 Ma zircon population. The analytical errors for individual analyses are typically too large ( $\sim 50$  Ma,  $2\sigma$ ) to distinguish subpopulations within a 100 Ma interval. However, multiple spots on particular grains permit improved analytical errors and more age detail. One younger grain (grain 20) yielded a weighted mean



$^{207}\text{Pb}/^{206}\text{Pb}$  age of  $1819 \pm 21$  Ma (95% confidence), MSWD = 1.2, probability of fit = 30%,  $n=3$  replicate analyses. This age is interpreted as the maximum age of deposition for member B of the Manitou Falls Formation. Grain 32, also part of this younger subset, gave a weighted mean

$^{207}\text{Pb}/^{206}\text{Pb}$  age of  $1823 \pm 18$  Ma, MSWD = 0.84, probability of fit = 47%, within error of the results from grain 20, from four replicate analyses.

### Z7462 Manitou Falls Formation, member D

Zircons from sample z7462 are generally well rounded compared to others from this study and vary widely in quality. Most grains are rounded prisms of varied clarity and colour, ranging from clear and colourless to dark brown and highly turbid. In BSE images, the clear, colourless, rounded prisms show few fractures. Most are unzoned; a few exhibit faint concentric zoning (see Fig. 8, grains 39, 81, 98). The darker, more turbid zircons generally are highly altered. Alteration appears as areas of lower BSE response (i.e. dark grey; see Fig. 8, grain 54 and 100), typically parallel to zoning. Highly altered zircons, such as grain 100 (Fig. 8), contain elevated levels of common Pb and were therefore avoided. However, it

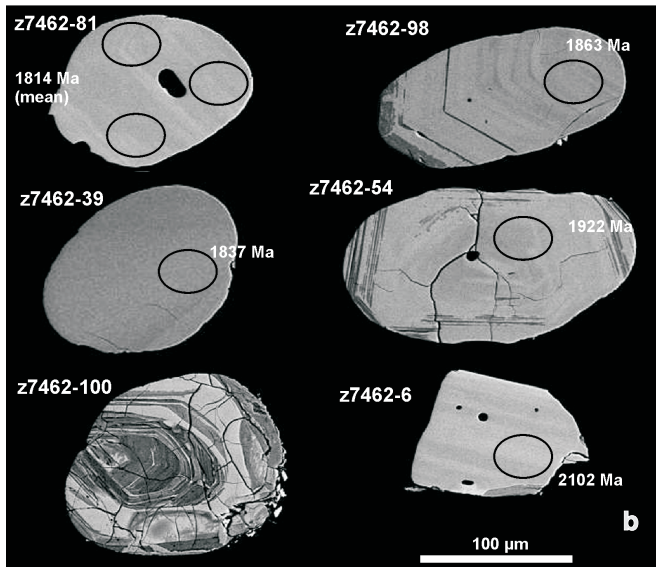
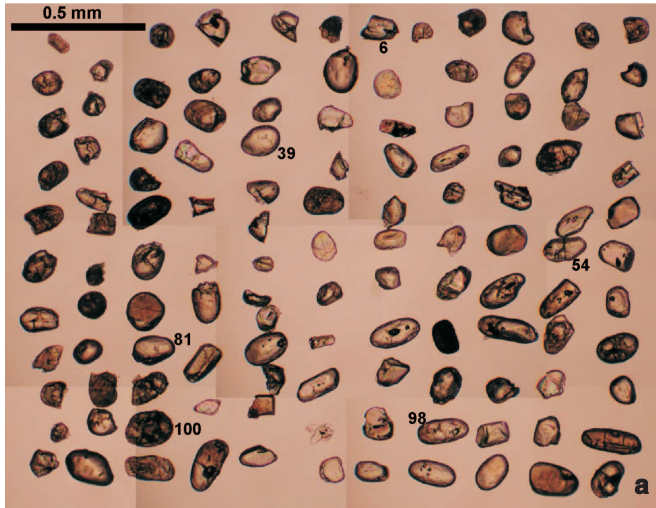


**Figure 8. a)** Transmitted-light image of the sample of detrital zircons picked from z7462 (Manitou Falls Formation, member D). Numbers in figure refer to the grain-identification numbers used during SHRIMP analysis and mentioned in the text. **b)** Backscattered-electron images of a representative selection of zircon grains. Ellipses represent approximate positions of SHRIMP analysis. Spot  $^{207}\text{Pb}/^{206}\text{Pb}$  ages are reported; see Table 2 for more details. The vertical and horizontal dark grey banding visible around the edges of grain 54 is an example of localized alteration. More pervasive alteration is present in grain 100, where all the dark grey material in the core and around the outer edge is altered, with only thin bands of unaltered zircon preserved.

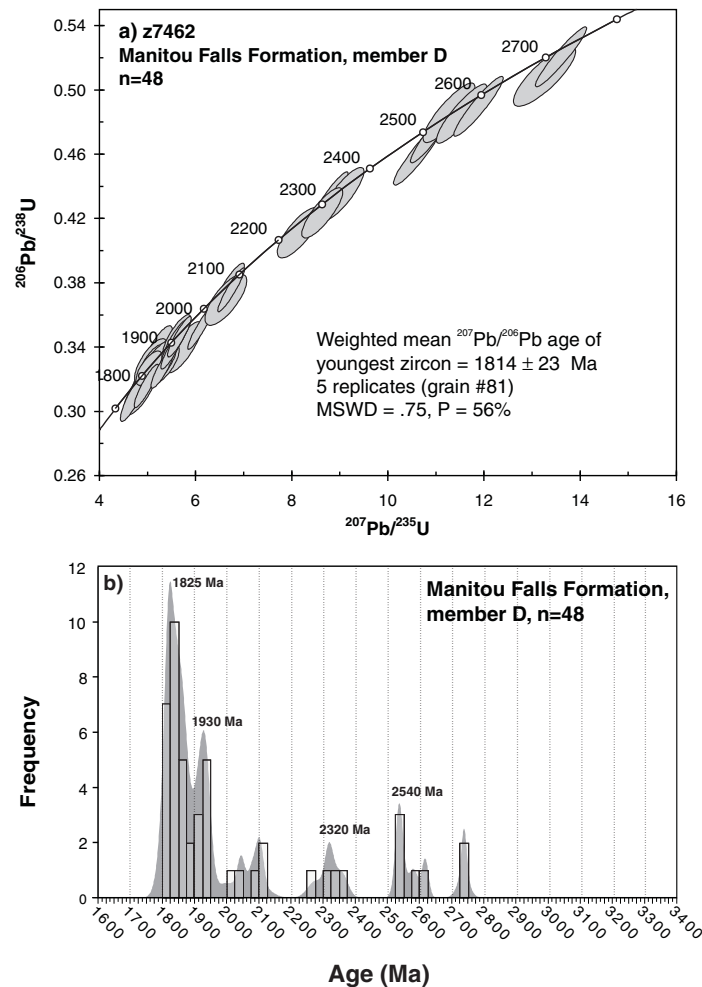


**Figure 9. a)** Concordia diagram of U-Pb results from sample z7462. Analyses discordant by >10% and replicate analyses were not plotted. Error ellipses are at  $2\sigma$ . **b)** Cumulative probability curve with overlain histogram. Bin width is 25 Ma, yielding 50% efficiency (Sircombe, 2000). Analyses discordant by >10% and replicate analyses were not included.

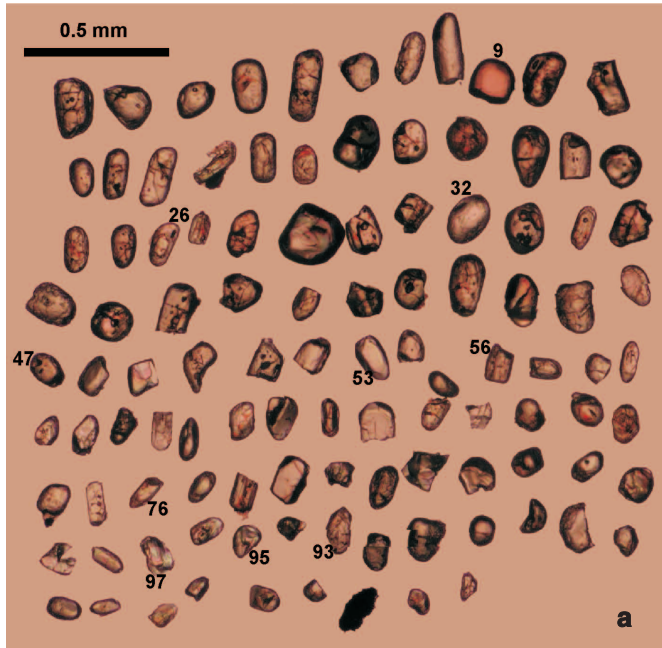
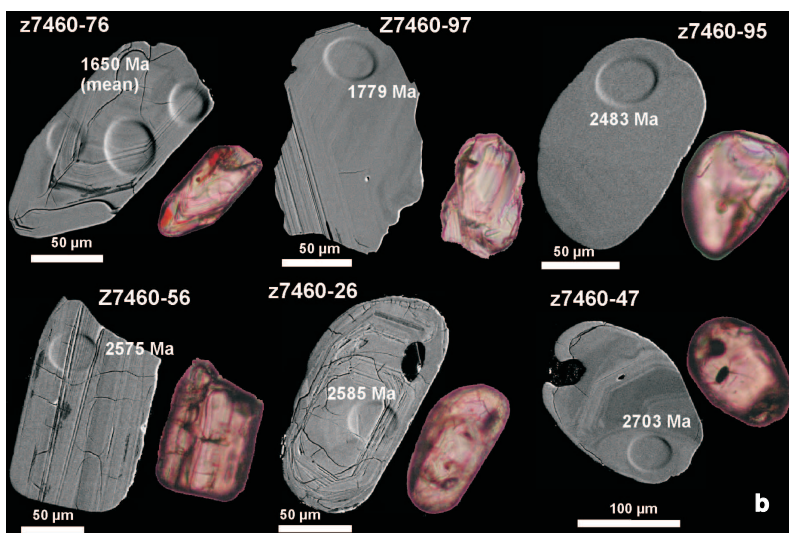


**Figure 10. a)** Transmitted-light image of the sample of detrital zircons picked from z7460 (Wolverine Point Formation, member B). Numbers in figure refer to the grain-identification numbers used during SHRIMP analysis and mentioned in the text. **b)** Post-analysis BSE and transmitted-light images of a representative selection of zircon grains, showing exact position of SHRIMP analysis. Spot  $^{207}\text{Pb}/^{206}\text{Pb}$  ages are reported; see Table 2 for more details. The zircons were etched using HF vapour to enhance the visibility of the zoning.



is possible to determine an age from unaltered regions of grains with localized alteration (*see* Fig. 8, grain 54). Although most of the zircons are strongly rounded, a small number of grains appear to be more angular and are perhaps fragments of larger zircons that were broken during the mineral separation procedure (*see* Fig. 8, grain 6).

Fifty-eight analyses on 52 different grains are presented in Table 2 and plotted on a concordia diagram and a cumulative probability curve with overlain histogram in Figure 9. Replicate analyses on individual grains, as well as results that were discordant by more than 10%, are not plotted. Most analyses ( $n=32$ ) fall between 1814 and 1940 Ma, in a bimodal distribution centred on 1825 Ma and 1930 Ma. The remaining concordant analyses range from 2004 Ma to 2738 Ma but extend up to ca. 3000 Ma if the discordant analyses are also

considered. Clusters of three or four analyses occur at roughly 2050 Ma, 2320 Ma and 2540 Ma. The younger ages (1814 to 1940 Ma) come from what appear to be good-quality, unzoned or concentrically zoned zircons. There is no distinct morphology or zoning pattern that defines the older zircons, although in general older zircons have patchy zonation and exhibit various extents of alteration.

In an attempt to better constrain the maximum age of deposition, multiple analyses were conducted on the two youngest grains, z7462-80 and -81. The weighted mean  $^{207}\text{Pb}/^{206}\text{Pb}$  age of grain 81 is  $1814 \pm 23$  Ma, MSWD = 0.75, probability of fit = 56%. The weighted mean  $^{207}\text{Pb}/^{206}\text{Pb}$  age of grain 80 is  $1819 \pm 20$  Ma, MSWD = 2.5, probability of fit =



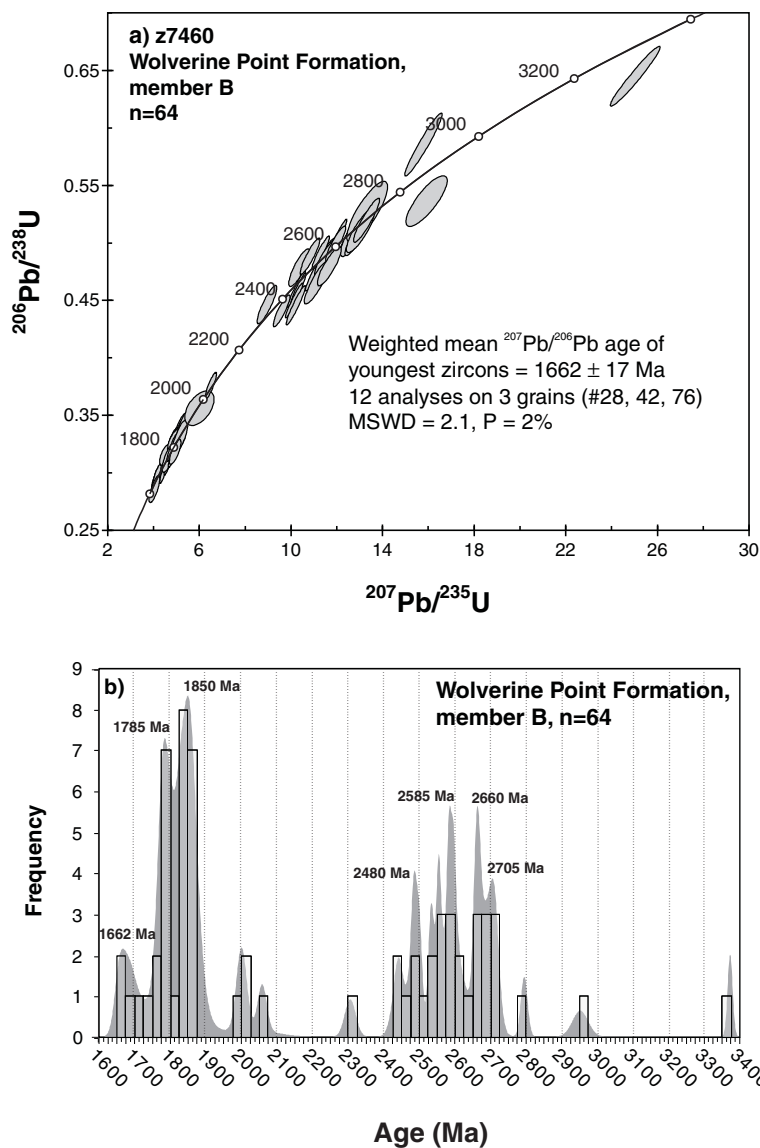


**Figure 11.**

**a)** Concordia diagram of U-Pb results from sample z7460. Replicate analyses were not plotted. Error ellipses are at  $2\sigma$ . **b)** Cumulative probability curve with overlain histogram. Bin width is 25 Ma, yielding 55% efficiency (Sircombe, 2000). Replicate analyses were not included.

8%, within error of the results from grain 81. Both these results are indistinguishable from the prominent Gaussian peak at ca. 1825 Ma.

### Z7460 Wolverine Point Formation, member B

Transmitted-light and BSE images of the zircons from the Wolverine Point Formation are presented in Figure 10. Backscattered-electron imaging was conducted both before and after SHRIMP analysis. The images shown in Figure 10 were taken after SHRIMP analysis (SHRIMP pits clearly visible) and after etching by brief exposure to hydrofluoric acid (HF) vapour. Etching with HF enhances the appearance of zoning in zircon by preferentially dissolving areas of zircon with greater amounts of radiation damage, i.e. higher U concentrations. The dominant zircon morphology from this sample is represented by rounded prisms of moderate quality. Grains generally are clear, colourless to pale brown; some contain numerous fractures and inclusions. Backscattered-electron

images reveal oscillatory zoning or no zoning (see Fig. 10, grains 76, 93). A minority of grains are very clear, with few inclusions or fractures, generally rounded, and exhibit very faint straight zoning in BSE images (see Fig. 10, grains 32, 53). A third group of zircons is composed of blocky fragments with good clarity and few inclusions or fractures (see Fig. 10, grains 97, 56). Backscattered-electron imaging of etched grains reveals finely spaced oscillatory zoning. The remaining zircons are pale brown to pink, large, equant to subequant, and well rounded, with faint, patchy zoning (see Fig. 10, grain 9).

A total of 73 analyses were conducted on 64 different grains; data are presented on concordia and cumulative-probability plots (Fig. 11). All results are within 7% of concordance; replicate analyses are not plotted. This sample shows the widest range of ages and the most complex distribution of detrital-zircon age modes of any of the five samples from this study. Apparent  $^{207}\text{Pb}/^{206}\text{Pb}$  ages range from 1650 to 3372 Ma. On the cumulative probability curve, the most

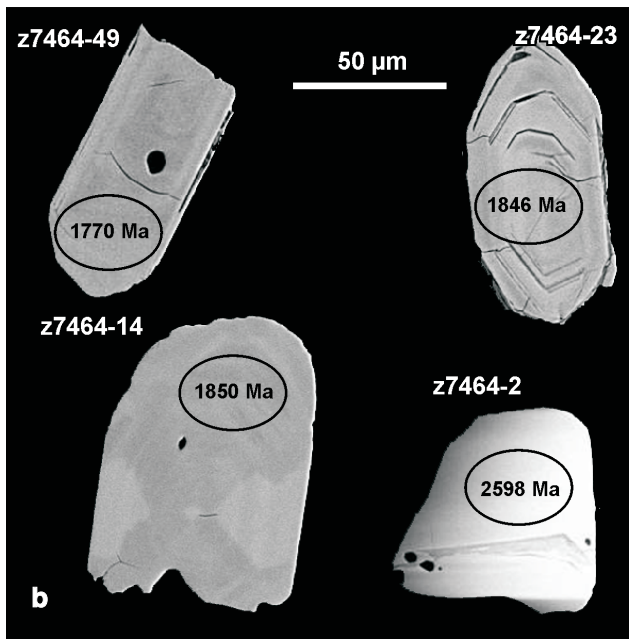
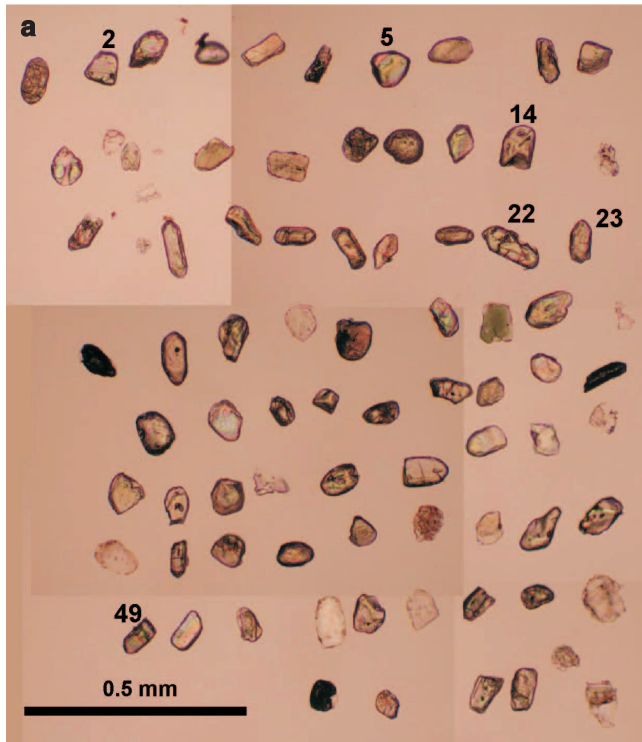


**Figure 12.** *a)* Transmitted-light image of the sample of detrital zircons picked from z7464 (Douglas Formation). Numbers in figure refer to the grain-identification numbers used during SHRIMP analysis and mentioned in the text. *b)* Backscattered-electron images of a representative selection of zircon grains. Ellipses represent approximate positions of SHRIMP analysis. Spot  $^{207}\text{Pb}/^{206}\text{Pb}$  ages are reported; see Table 2 for more details.

prominent modes are centred at 1785 Ma and 1850 Ma, grouping 25 analyses altogether. Another group of 26 grains records a broad range of ages between 2436 and 2713 Ma, with slightly more prominent clusters at ca. 2585 Ma and 2650–2725 Ma. Three other grains yielded ages of 2794, 2952 and 3372 Ma. Most interestingly, three grains (28, 42 and 76) yielded ages of ca. 1660 Ma, roughly 100 Ma younger than any other detrital zircons analyzed in this study. Replicate analyses were conducted on each of these grains; the weighted mean  $^{207}\text{Pb}/^{206}\text{Pb}$  age for each young grain is given in Table 2. The ages of these three grains are unique; all grains are very similar geochemically ( $U = 130\text{--}260$  ppm,  $\text{Th}/U = 0.6\text{--}0.9$ ), and as such we can consider them as a distinct single population. The weighted mean of all analyses (including replicates,  $n=12$ ) is  $1662 \pm 17$  Ma,  $\text{MSWD} = 2.1$ , probability of fit = 2%; this constrains the maximum age of deposition of the Wolverine Point Formation. Grain morphology does not correlate with age in any straightforward way; for example, the youngest grains are also well rounded.

### **Z7464 Douglas Formation**

The Douglas Formation is the uppermost unit from the Athabasca Basin from which a sample was analyzed for detrital zircon geochronology. Zircon recovery from this fine-grained quartz arenite was very low, and grains are small relative to those from the other samples (typically 50 µm across). The transmitted-light image in Figure 12 shows all of the recovered zircons, as well as a number of grains with low relief that are not zircon. Approximately one-third of the mounted zircons are subrounded prisms whose quality varies from good to poor. They are commonly fractured, and some contain inclusions. In BSE images, these zircons exhibit oscillatory zoning and areas showing various degrees of alteration that parallel the zoning (*see* Fig. 12, grains 22, 23, 49). Another third of the zircon grains are of higher quality, with few fractures or inclusions. These are typically well rounded, subequant, clear and colourless. In BSE images, most of these zircons are unzoned; a few exhibit faint sector zoning (*see* Fig. 12, grains 5, 14). The remainder of the zircons are irregular fragments, perhaps from larger grains. In BSE images, these zircons exhibit either irregular or concentric zoning; a few are unzoned (*see* Fig. 12, grain 2).

Due to the limited zircon yield, it was only possible to conduct 40 analyses on 37 different grains. The data are presented in the concordia diagram and cumulative probability curve in Figure 13. Results that are discordant by more than 10% were not plotted ( $n = 8$ ); nor were replicate analyses. The cumulative probability curve of the Douglas Formation sample is quite similar to that of the underlying Wolverine Point Formation. The prominent modes are almost identical at 1780 Ma and 1850 Ma. A loose grouping of seven older grains yield concordant ages between 2443 and 2691 Ma, the same age range obtained for older zircons from the Wolverine Point formation. Absent are the rare ancient zircons (2.8–3.4 Ga), and no grains are younger than 1775 Ma. The maximum age of deposition cannot be further constrained than that obtained for the underlying Wolverine Point Formation (1660 Ma).

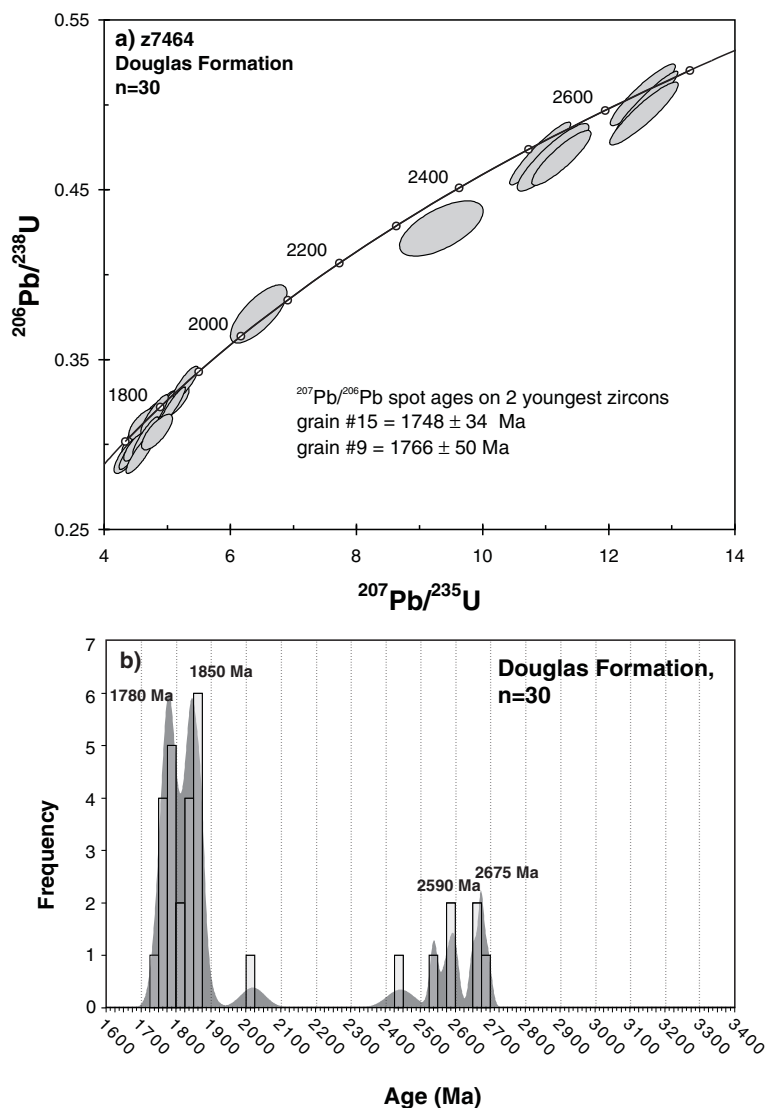


**Figure 13.**

a) Concordia diagram of U-Pb results from sample z7464. Analyses discordant by >10% and replicate analyses were not plotted. Error ellipses are at 2σ. b) Cumulative probability curve with overlain histogram. Bin width is 25 Ma, yielding 50% efficiency (Sircombe, 2000). Analyses discordant by >10% and replicate analyses were not included.

**Table 3.** Summary of detrital-zircon SHRIMP U-Pb results for the Athabasca Basin.

Sample	Unit	Stratigraphic position	No. of analyses	No. of grains	Youngest zircon	Prominent age modes	
z7464	Douglas Fm	TOP	40	37	1765-1775 Ma	1780, 1850, 2590, 2675 Ma	
z7460	Wolverine Point Fm	↑	73	64	1662 ± 17 Ma	1660, 1785, 1850, 2480, 2585, 2660, 2705 Ma	
z7462	Manitou Falls Fm, member D		58	52	1814 ± 23 Ma	1825, 1930, 2320, 2540 Ma	
z7465	Manitou Falls Fm, member B		72	62	1819 ± 21 Ma	1850, 2090, 2515, 2575 Ma	
z7461	Fair Point Fm		BOTTOM	67	61	1810 ± 15 Ma	1900, 2520, 2585, 2610 Ma

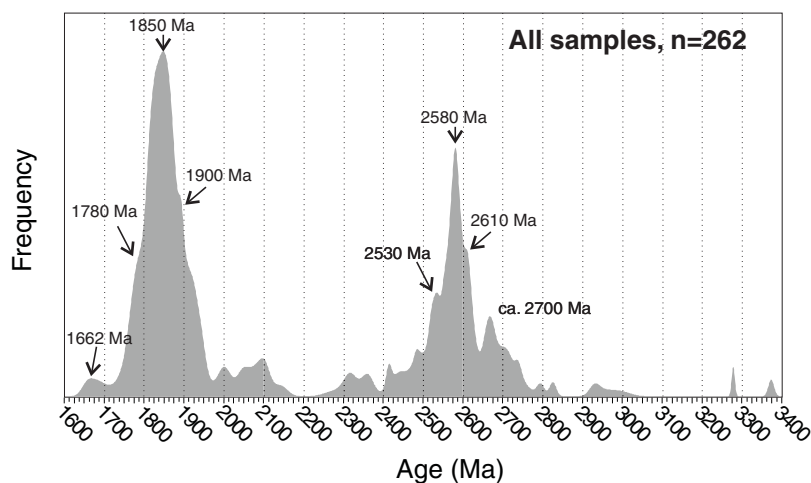
## CONCLUSIONS

Detrital-zircon SHRIMP U-Pb results for five sandstone samples from the Athabasca Group are summarized in Table 3. Figure 14 is a cumulative probability curve encompassing the compiled results from all five samples and illustrates prominent age modes for the Athabasca Basin at 1780 Ma, 1850 Ma, 1900 Ma, 2530 Ma, 2580 Ma, 2610 Ma, and ca. 2700 Ma.

In the case of some specimens, the age of the youngest detrital zircon may be interpreted as being close to the age of deposition (e.g. 1660 Ma zircons in the Wolverine Point Formation). The youngest zircon in the basal Fair Point Formation indicates that sedimentation began in the Athabasca Basin sometime after 1810 Ma. However, geochronological data from underlying basement rocks suggest tighter constraints. Further discussion and interpretation of these results will be presented in a paper by Rainbird and others to be published in the EXTECH IV final volume.

**Figure 14.**

Cumulative probability curve of compiled SHRIMP U-Pb detrital zircon results for the five samples of Athabasca Basin sandstone studied here.



## ACKNOWLEDGMENTS

The results presented in this paper stem from GSC Geochronology Project P231 as a contribution to EXTECH IV Subproject 11 (GSC Project PS1018), which is supported in part by the Targeted Geoscience Initiative. Samples were collected by Paul Ramaekers (Ramaekers' archive sample relabelled as 02JP-15a), Darrel Long (RAT01-MF1), Gary Yeo (02JP-20a), and Charlie Jefferson (02JP12,13,14). Critical review was carried out by Charlie Jefferson.

## REFERENCES

### Armstrong, R.L. and Ramaekers, P.

1985: Sr isotopic study of Helikian sediment and diabase dikes in the Athabasca Basin, northern Saskatchewan; *Canadian Journal of Earth Sciences*, v. 22, p. 399–407.

### Cumming, G.L., Krstic, D., and Wilson, J.A.

1987: Age of the Athabasca Group, northern Alberta; *Geological Association of Canada – Mineralogical Association of Canada Annual Meeting, Program with Abstracts*, v. 12, p. 35.

### Jefferson, C.W., Delaney, G., and Olson, R.A.

2002: EXTECH IV Athabasca uranium multidisciplinary study: Mid-year 2002-03 overview and impact analysis; *in Summary of Investigations 2002, Volume 2*, Saskatchewan Geological Survey, Saskatchewan Industry and Resources, Miscellaneous Report 2002-4.2, Paper D-1, 12 p. (CD-ROM)

### Kotzer, T.G. and Kyser, T.K.

1995: Petrogenesis of the Proterozoic Athabasca Basin, northern Saskatchewan, Canada, and its relation to diagenesis, hydrothermal uranium mineralization and paleohydrology; *Chemical Geology*, v. 120, p. 45–89.

### Ludwig, K.R.

2001: User's manual for Isoplot/Ex rev. 2.49: a Geochronological Toolkit for Microsoft Excel; Berkeley Geochronology Center, Special Publication, 1a, 55 p.

### Ramaekers, P., Yeo, G.M., and Jefferson, C.W.

2001: Preliminary overview of regional stratigraphy in the late Paleoproterozoic Athabasca Basin, Saskatchewan and Alberta; *in Summary of Investigations 2001, Volume 2*, Saskatchewan Geological Survey, Saskatchewan Energy and Mines, Miscellaneous Report 2001-4.2b. (CD-ROM)

### Sircombe, K.

2000: The usefulness and limitations of binned frequency histograms and probability density distributions for displaying absolute age data; *Geological Survey of Canada, Current Research 2000-F2*, 11 p.

### Stern, R.A.

1997: The GSC Sensitive High Resolution Ion Microprobe (SHRIMP): analytical techniques of zircon U-Th-Pb age determinations and performance evaluation; *in Current Research 1997-F*; Geological Survey of Canada, p. 1–31.

### Stern, R.A., and Amelin, Y.

2003: Assessment of errors in SIMS zircon U-Pb geochronology using a natural zircon standard and NIST SRM 610 glass; *Chemical Geology*, v. 197, p. 111–146.

### Thomas, D.J., Jefferson, C.W., Yeo, G.M., Card, C., and Sopuck, V.

2002: Introduction; *in Trip A1: The Eastern Athabasca Basin and its Uranium Deposits*, (ed.) N. Andrade, G. Breton, C.W. Jefferson, D.J. Thomas, G. Tourigny, S. Wilson, and G.M. Yeo; Geological Survey of Canada – Mineralogical Association of Canada, Saskatoon 2002 Field Trip Guide, p. 1–22.

Geological Survey of Canada Project PS1018